

Ease.ml/snoopy: Towards Automatic Feasibility Study for Machine Learning Applications

Cedric Renggli^{*,†}, Luka Rimanic^{*,†}, Luka Kolar^{*,†}, Nora Hollenstein[†], Wentao Wu[§], Ce Zhang[†]

[†]ETH Zurich, [§]Microsoft Research

[†]{cedric.renggli, luka.rimanic, luka.kolar, noraho, ce.zhang}@inf.ethz.ch, [§]wentao.wu@microsoft.com

ABSTRACT

In our experience of working with domain experts who are using today’s AutoML systems, a common problem we encountered is what we call “*unrealistic expectations*” – when users are facing a very challenging task with noisy data acquisition process, whilst being expected to achieve startlingly high accuracy with machine learning (ML). Consequently, many computationally expensive AutoML runs and labour-intensive ML development processes are predestined to fail from the beginning. In traditional software engineering, this problem is addressed via a *feasibility study*, an indispensable step before developing any software system. In this paper, we present ease.ml/snoopy with the goal of preforming an *automatic feasibility study before building ML applications or collecting too many samples*. A user provides inputs in the form of a dataset, which is representative for the task and data acquisition process, and a quality target (e.g., expected accuracy > 0.8). The system returns its deduction on whether this target is achievable using ML given the input data. We approach this problem by estimating the *irreducible error* of the underlying task, also known as Bayes error. The technical key contribution of this work is the design of a practical Bayes error estimator. We carefully evaluate the benefits and limitations of running ease.ml/snoopy prior to training ML models on too noisy datasets for reaching the desired target accuracy. By including the automatic feasibility study into the iterative label cleaning process, users are able to save substantial labeling time and monetary efforts.

1 INTRODUCTION

Modern software development is typically guided by software engineering principles that have been developed and refined for decades [38]. Even though such principles are yet to come to fruition when it comes to the development of machine learning (ML) applications, in recent years we have witnessed a surge of work focusing on ML usability through supporting efficient ML systems [20, 21, 41], enhancing developer’s productivity [1, 2, 19], and finally supporting the ML application development process itself [14, 18, 22, 23, 25, 28, 29, 39]. We believe that, in the future, the development of ML applications will follow a set of well-defined principles and processes, similar to how software engineering principles have been guiding the software engineering process for years.

Calls for a Feasibility Study of ML. In this paper, we focus on one specific “failure mode” that we frequently witness whilst working with a range of domain experts, which we call “*unrealistic expectations*.” We often see developers that work on challenging tasks with a dataset that is too noisy to meet the unrealistically high expectations on the accuracy that can be achieved with ML. In such

a setting, approaches relying on ML are predestined to fail to meet the expectations, turning it into a costly business, both in terms of wasted development time and resources for gathering more data and training ML models.

In an ideal world, such problems should be caught *before* a user commits significant amount of resources to train or tune ML models. In fact, if one can afford a *human ML consultant*, this is often the very first step of the service. Such a consultant would analyze the representative dataset for the defined task and assess the *feasibility* of the target accuracy. If the consultant *concludes* that the target is not achievable, one can then explore alternative options by refining the dataset, the acquisition process, or exploring different task definitions. Borrowing the term from classic software engineering, we believe that this *feasibility study* is crucial to the usability of future ML systems for application developers. In this paper, we ask: *Can we automate this feasibility study process?*

Scope and Targeted Use Cases. As one of the first attempts towards understanding this problem, this paper by no means provides a complete solution. Instead, we scope ourselves to a very specific application scenario and provide a deep understanding both theoretically and empirically. We hope that our exploration of this specific use case can inspire future endeavors on what we believe to be an exciting research direction.

Specifically, we focus on the case in which a user has access to a dataset \mathcal{D} , large enough to be representative for the underlying task. However, the dataset is noisy in its labels, probably caused by (1) the inherent noise of the data collection process such as *crowd sourcing* [6, 7, 13, 36], or (2) *bugs* in the data preparation pipeline (which we actually see quite often in practice). The user has a target accuracy α_{target} and can spend time and money on two possible operations: (1) manually clean up some labels in the dataset, or (2) find and engineer suitable ML models, manually or automatically. Without any feasibility study, we often see users directly deploying an expensive AutoML engine for hours or even days, or jumping into the loop of trying different ML solutions based on a dataset that is too noisy to reach the target accuracy α_{target} in the first place. The goal of a feasibility study is to *automatically provide an estimate on the best possible accuracy that any ML model can achieve for the task represented by the dataset*.

Strawman Strategy: A Cheap Proxy Model. A natural, rather trivial approach to the above problem is to run a cheap proxy model, e.g., logistic regression, over \mathcal{D} , to get an accuracy α_{proxy} , and use it to produce an estimator α_{est} (with $\alpha_{\text{est}} > \alpha_{\text{proxy}}$ to factor in the fact that we are using a cheap proxy model). Although one could simply take this heuristic and make ad-hoc design decisions to have a system, there is a range of fundamental questions that we need to

understand in order to have a principled treatment of this problem: *What is the best choice of the proxy model? What is a theoretically sound way of adjusting the gap between α_{proxy} and α_{est} ? Which optimizations can we conduct to make our estimation faster and more accurate?* As we will see, understanding these questions is far from trivial, and giving a principled treatment to these questions will lead to a system that outperforms ad-hoc baselines.

Feasibility Study and BER: Theory vs. Practice. From a theoretical perspective, our way of performing a feasibility study is not new; rather it connects to a decade-old ML concept known as the Bayes error rate (BER) [8], the “irreducible error” of a given task corresponding to the error rate of a *Bayes optimal classifier*. Estimation of the BER has been studied intensively for almost half a century by the ML community [3, 4, 9–11, 24, 33]. Some of these works directly estimate the BER, whilst others rely on a proxy model (e.g., k-nearest neighbor classifiers) and principled ways to calculate α_{est} with α_{proxy} . However, most, if not all, of these works are mainly theoretical, evaluated on either synthetic and/or very small datasets of often small dimensions. *How can we bring the theoretical understanding and results to practice?* As we will see, this requires not only new algorithmic and theoretical developments, but also careful design and optimization of data systems.

Summary of Contributions. We present `ease.ml/snoopy`, an automatic feasibility study system for machine learning. Following previous theoretical endeavors, `ease.ml/snoopy` models the problem of feasibility study as estimating a *lower bound* of the BER. However, to enable such a functionality in a real-world system applied to realistic datasets, we need to take a system’s perspective and study practical estimators of the BER. These comprise the key technical contributions of this work, summarized as follows.

C1. Systems Abstractions and Designs. As one of the first systems for automatic feasibility study of ML development, `ease.ml/snoopy` models the problem of feasibility study as estimating a *lower bound* of the Bayes error rate. Users provide `ease.ml/snoopy` with a dataset representative for their ML task, along with a target accuracy. The system then outputs a binary signal assessing whether the target accuracy is realistic or not. Being aware of failures (false-positives and false-negatives) in the binary output of our system, which we carefully outline and explain in this paper, we support the users of our system in deciding on whether to “trust” the output of `ease.ml/snoopy` by providing additional numerical and visual aids. We show an end-to-end use case of incrementally improving the label quality of an initially too noisy dataset until the desired target accuracy is reachable, enabling substantial savings in terms of money spent on computation and human annotators.

The technical core is a practical BER estimator. We propose a simple, but novel approach, which consults a collection of different Bayes error estimators and aggregates them through taking the minimum. We provide a theoretical analysis on the regimes under which this aggregation function is justified, reflecting the current landscape of existing estimators.

C2. Design Space Exploration. We explore the design space in order to understand different Bayes error estimators and how they

fit into `ease.ml/snoopy`. This is a challenging task — even comparing different BER estimators without knowing the ground truth is an open problem. We tackle this in two parts, by first proposing a novel practical framework for comparing different BER estimators and then systematically evaluating a range of seven existing Bayes error estimators on well-established benchmark datasets. To the best of our knowledge, this is the first large-scale study of BER estimators on real-world data, an effort that, we hope, can open up future research endeavors. Due to space constraints, we only summarize the insights in the main body and provide more details in the supplementary material.

In summary, we find that a family of BER estimators based on the k-nearest-neighbor (kNN) classifier, which also takes advantage of a collection of pre-trained feature embeddings, outperforms other estimators in terms of accuracy of the estimation and computational performance. The convergence behaviour of this family of estimators was covered in our theoretical paper [32]. This work is the first to test its utility as BER estimators.

C3. System Optimizations. We then describe the implementation of `ease.ml/snoopy`, with optimizations that improve its performance. We describe a system implementation that uses *successive-halving* [15], a part of the textbook Hyperband algorithm [19], to balance the resources spent on different estimators. This already outperforms naive approaches significantly. We further improve on this method by taking into consideration the convergence curve of estimators, fusing it into a new variant of successive-halving. Moreover, noticing the iterative nature of the interaction model between `ease.ml/snoopy` and the user, we take advantage of the property of kNN classifiers and implement an incremental version of the system. For application scenarios in which a user cleans some labels, `ease.ml/snoopy` is able to provide feedback in real-time (0.2 ms for 10K test samples and 50K training samples).

Limitations. In this paper, we focus on the challenging endeavor of estimating the *irreducible error* for the task definition and data acquisition process. We by no means provide a conclusive solution to preventing unrealistic or very costly endeavors of training ML models with finite data. We view our contribution as a first step towards a practical treatment of this problem, which is the key for enabling an automatic feasibility study for ML. As a result, in Section 2 we carefully describe limiting assumptions on the data distributions, as well as failure causes and cases of the current system and method, presented in Section 3 and Section 5 respectively, hoping that this can stimulate future research from the community.

2 PRELIMINARIES

In this section, we give a short overview over the technical terms and the notation used throughout this paper. Let \mathcal{X} be the feature space and \mathcal{Y} be the label space, with $C = |\mathcal{Y}|$. Let X, Y be random variables taking values in \mathcal{X} and \mathcal{Y} , respectively. We denote their joint distribution by $p(X, Y)$ and write $p(x, y) = p(X=x, Y=y)$. We define $\eta_y(x) = p(y|x)$ when $C > 2$, and $\eta(x) = p(1|x)$ when $C = 2$, in which case we assume $\mathcal{Y} = \{0, 1\}$.

Bayes Error. *Bayes optimal classifier* is the classifier that achieves the lowest error rate among all possible classifiers from \mathcal{X} to \mathcal{Y} , with respect to p . Its error rate is called the *Bayes error rate (BER)*

and we denote it by $R_{X,Y}^*$, often abbreviated to R_X^* when Y is clear from the context. It can be expressed as

$$R_X^* = \mathbb{E}_X [1 - \max_{y \in \mathcal{Y}} \eta_y(x)]. \quad (1)$$

When examining the estimators, we only consider methods capable of estimating the Bayes error for multi-class classification problems ($C \geq 2$), and divide them into three categories, based on different parts of Equation 1. In Section 3.1, where we describe the design space of our system, we distill each of these groups in detail. Our main choice for the BER estimator is based on the accuracy of the nearest-neighbor classifier (i.e., kNN with $k = 1$) on top of *pre-trained* feature transformations. We show that this leads to a powerful estimator that outperforms all other methods in terms of practicality, scalability, and performance, making it perfectly suitable from the system’s perspective.

One fundamental limitation of the above formulation is that it assumes that both the training and validation data are drawn i.i.d. from the *same* distribution, which does not need to hold in practice, especially when applying data programming or weak supervision techniques [27]. It will be interesting to explore this aspect in the future, starting more from the theoretical angle.

2.1 K-Nearest-Neighbor (kNN) Classifier

Given a training set $\mathcal{D}_n := \{(x_1, y_1), \dots, (x_n, y_n)\}$ and a new instance x , let $(x_{\pi(1)}, \dots, x_{\pi(n)})$ be a reordering of the training instances by their distances from x , based on some metric (e.g., Euclidean or cosine dissimilarity). The *kNN classifier* $h_{n,k}$ and its *n-sample error rate* $(R_X)_{n,k}$ are defined by

$$h_{n,k}(x) = \arg \max_{y \in \mathcal{Y}} \sum_{i=1}^k \mathbf{1}_{\{y_{\pi(i)}=y\}}, \quad (R_X)_{n,k} = \mathbb{E}_{X,Y} \mathbf{1}_{\{h_{n,k}(X) \neq Y\}},$$

respectively. The *infinite-sample error rate* of kNN is given by $(R_X)_{\infty,k} = \lim_{n \rightarrow \infty} (R_X)_{n,k}$. Cover and Hart [8] derived the following fundamental and well-known relationship between the nearest neighbor algorithm and the BER (under very mild assumptions on the underlying probability distribution):

$$(R_X)_{\infty,1} \geq R_X^* \geq \frac{(R_X)_{\infty,1}}{1 + \sqrt{1 - \frac{C(R_X)_{\infty,1}}{C-1}}}. \quad (2)$$

Determining such a bound for $k > 1$ and $C > 2$ is still an open problem, and in this work we mainly focus on $k = 1$.

kNN Classifier and Feature Transformations. Since our estimator will combine the kNN algorithm with pre-trained feature transformations, also called *embeddings*, such as those publicly available, we need to understand the influence of such transformations. In our theoretical companion to this paper [32], we provide a novel study of the behavior of a kNN classifier on top of a feature transformation, in particular its convergence rates on *transformed* data, previously known only for the *raw* data.¹ We prove the following theorem, recalling that a real-valued function g is *L-Lipschitz* if $|g(x) - g(x')| \leq L\|x - x'\|$, for all x, x' , and defining $\mathcal{L}_g(f) := \mathbb{E}_X [(g \circ f)(X) - \eta(X)]^2$.

¹We restrict ourselves to $C = 2$, as usual in theoretical results about the convergence rates of a kNN classifier.

THEOREM 2.1 (RIMANIC ET AL. [32]). *Let $X \subseteq \mathbb{R}^D$ and $\tilde{X} \subseteq \mathbb{R}^d$ be bounded sets, and let (X, Y) be a random vector taking values in $X \times \{0, 1\}$. Let $g: \tilde{X} \rightarrow \mathbb{R}$ be an L_g -Lipschitz function. Then for all transformations $f: X \rightarrow \tilde{X}$,*

$$\mathbb{E}_n [(R_{f(X)})_{n,k}] - R_X^* = O\left(\frac{1}{\sqrt{k}}\right) + O\left(L_g \left(\frac{k}{n}\right)^{1/d}\right) + O\left(\sqrt[4]{\mathcal{L}_g(f)}\right). \quad (3)$$

Motivated by the usual architecture of trained embeddings, in Theorem 2.1 one should think of g as a softmax prediction layer with weights w , which allows taking $L_g = \|w\|^2$. Equation 3 shows that there is a trade-off between the improved convergence rates (in terms of L_g and d) and the bias that does not depend on the properties of the kNN algorithm, introduced by the transformation.

3 DESIGN AND IMPLEMENTATION

We present the design and implementation of `ease.ml/snoopy`, providing an overview of the workflow and theoretical analysis. A high-level overview of our system is given in Figure 1.

Functionality. `ease.ml/snoopy` interacts with users in a simple way. The user provides an input dataset that is representative for the classification task at hand, along with a target accuracy α_{target} . The system then estimates the “highest possible accuracy” that an ML model can achieve, and outputs a binary signal — **REALISTIC**, if the system deduces that this target accuracy is achievable; **UNREALISTIC**, otherwise. We note that `ease.ml/snoopy` does not provide a model that can achieve that target, only its belief on whether the target is achievable, using an *inexpensive* process. Furthermore, the goal of `ease.ml/snoopy` is *not* to provide a perfect answer on feasibility, but to give information that can guide and help with the decision-making process — the signal provided by the system may as well be wrong, for the following reasons.

Interaction Model. The binary signal of `ease.ml/snoopy` given to a user is often correct, but not always. We now dive into the user’s and `ease.ml/snoopy`’s interaction upon receiving the signal.

*The Case When `ease.ml/snoopy` Reports **REALISTIC**.* In general, one should trust the system’s output when it reports the target to be realistic, and proceed to running AutoML. In theory, `ease.ml/snoopy` could be wrong due to (1) a lower bound that is known not to be always tight, or (2) the fact that the estimators are predicting asymptotic values. However, in our experiments we do not observe either case and this behavior. Even if this were the case, we expect (2) to be the dominating reason, in which case gathering more data for the task at hand and running AutoML on this larger dataset should confirm the system’s prediction.

*The Case When `ease.ml/snoopy` Reports **UNREALISTIC**.* In this case, our experiments showed that the system’s output is also trustworthy — with more caution. Under reasonable computational resources², `ease.ml/snoopy` is often correct in preventing unrealistic expectations for a varying amount of label noise. Nonetheless, there are two possible reasons for making wrong predictions in this manner: (1) either the data is not representative enough for the task (i.e.,

²For instance: reproducing the state-of-the-art model performance for well-established benchmark datasets is often a highly non-trivial task.

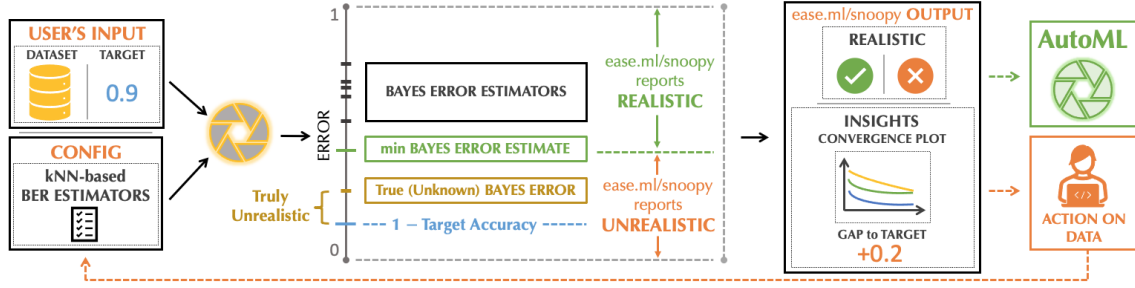


Figure 1: Overview of ease.ml/snoopy.

users might need to acquire more data), or (2) the transformations applied in order to reduce the feature dimension, or to bring raw features into a numerical format in the first place (e.g., from text), increased the BER.³ We note that (1) and (2) are complementary to each other. Even though estimating the BER on raw features (if applicable) prevents (2) from happening, having “better” transformations can lower the number of samples required to accurately estimate the BER. In an ideal world, one could rule out (1) by checking whether the BER estimator converged on raw features on the given number of samples. That is why ease.ml/snoopy provides insights in terms of convergence plots, in order to help users understand the *source* of predicting UNREALISTIC, and increase the confidence in the system’s prediction.

Bayes Error Estimation. The core component of ease.ml/snoopy is a BER estimator, which estimates the irreducible error of a given task. The task of estimating BER is inherently difficult and a usable system needs to contain practical compromises. The key design decision of ease.ml/snoopy is to consult a collection of estimators and aggregate them in a meaningful way. Specifically, given a collection of estimators \mathcal{R}_X , ease.ml/snoopy takes their minimum in view of $\hat{S}_X := \min_{R \in \mathcal{R}_X} \hat{R}$. Finally, the system’s output is

$$\begin{aligned} &\text{REALISTIC,} && \text{if } \hat{S}_X \leq 1 - \alpha_{\text{target}}, \\ &\text{UNREALISTIC,} && \text{otherwise.} \end{aligned}$$

Additional Guidance. To support users of ease.ml/snoopy in deciding whether to “trust” the output of the system, regardless of the outcome, additional information is provided. It comes in the form of (a) the estimated BER lower bound and, thus, the *gap* between the projected accuracy and the target accuracy, and (b) the convergence plots indicating the estimated BER value with respect to increased number of training samples over all deployed BER estimators (c.f., Figures 11-13 in the supplementary material).

Discussion. At first glance, our system might seem like a “light-weight AutoML system,” which runs a collection of fast models (e.g., kNN classifiers) and takes the minimum to get the best possible classifier accuracy. We emphasize the difference — the accuracy of an AutoML system always corresponds to a concrete ML model that can achieve this accuracy; however, a BER estimator does not provide this concrete model. That is, ease.ml/snoopy does not construct a model that can achieve \hat{S}_X . This key difference between

AutoML and feasibility study makes the latter inherently more computationally efficient, with almost instantaneous re-running, which we will further illustrate with end-to-end experiments in Section 5.

3.1 Design Space

To construct each individual Bayes error estimator in \mathcal{R}_X , we consider two largely orthogonal dimensions: (1) the algorithm depicting an estimator, and (2) the feature space over which an estimator is applied. We now describe these notions, but leave the detailed empirical exploration for the next section.

BER Estimation Algorithms. On the algorithm side, we divide existing BER estimators into three groups, each of them estimating different parts of Equation 1, highlighted in Equation 6 in the supplementary material. In this section we provide an overview of existing estimators, whereas individual details on each method can be found in Section B of the supplementary material.

- **Density Estimators:** *DE-kNN* [12] and *KDE* [11] are based on estimating the per-class posterior η_y , for all $y \in \mathcal{Y}$.
- **Divergence Estimator:** *GHP* [33] is based on the generalized Henze-Penrose divergence between every pair of η_i and η_j , yielding a provably valid estimator of the BER in the asymptotic regime. It is similar to kNN-LOO in terms of computational complexity.
- **kNN Classifier Accuracy:** *1NN-kNN* [9], *kNN-Extrapolation* [35], *kNN-LOO* (for a fair comparison with non-scalable methods), and *kNN* are all based on the accuracy of a kNN classifier. Here kNN and kNN-LOO are inspired by Cover and Hart [8], recalling that such an expression exists for $C > 2$ only when $k = 1$, using the validation error of a 1NN classifier $(R_X)_{n,1}$ after normalizing:

$$\hat{R}_{X,h_{n,1}} := \frac{(R_X)_{n,1}}{1 + \sqrt{1 - \frac{C(R_X)_{n,1}}{C-1}}}. \quad (4)$$

Feature Space. Each of the above algorithms can be applied to the raw feature space, but most of them will suffer from the curse of dimensionality. To surpass this, practitioners apply dimension reduction algorithms (e.g., PCA), yielding some improvements [33]. Recently, pre-trained feature embeddings have become increasingly popular on platforms such as TensorFlow Hub, PyTorch Hub, and HuggingFace Transformers. Applying these embeddings and a BER estimator on top of them increases the space and quality of BER estimators, adding an additional dimension to the design space.

3.2 Taking the Minimum Over Estimators

Given a collection of Bayes error estimators as a subset of the previously defined design space, ease.ml/snoopy aggregates them

³We have shown in our theoretical companion [32] that any deterministic transformation can only increase the BER.

by taking the minimum. We now analyze this simple aggregation rule and depict the regimes under which it is justified.

The fundamental difficulties are caused by the fact that we only have access to estimators based on a dataset with *finite* number of samples n . Let \widehat{R} be any estimator of the lower bound of the BER on X (for example the estimator that uses the 1NN classifier). This is referred to as the *asymptotic* version, whereas we denote its n -sample version by \widehat{R}_n . Most, if not all, existing estimators are connected to the BER in the asymptotic regime, either through a consistency result or through the lower bound itself. Therefore, there are two main quantities that explain the finite-sampled estimators: (1) the *bias* of the estimator, defined by $\Delta_X(\widehat{R}) = \widehat{R} - R_X^*$, and (2) the *n-sampled distance* from the asymptotic regime, defined by $\delta_n(\widehat{R}) = \widehat{R}_n - \widehat{R}$. Informally, bias reflects the quality of the estimator, whereas n -sampled distance depicts whether the finite-sampled estimator converged to its asymptotic version. Understanding each of these quantities provides the basis for measuring the *n-sample gap*, defined by $\mathcal{G}_{X,n}(\widehat{R}) := |R_X^* - \widehat{R}_n|$. With the goal of checking whether taking the minimum over all estimators is close to being optimal, for a collection of BER estimators \mathcal{R}_X we define

$$\mathcal{G}_{X,n}^{\min}(\mathcal{R}_X) := \mathcal{G}_{X,n}(\arg \min_{\widehat{R} \in \mathcal{R}_X} \widehat{R}) - \min_{\widehat{R} \in \mathcal{R}_X} \mathcal{G}_{X,n}(\widehat{R}).$$

LEMMA 3.1. *Let \mathcal{R}_X be a collection of BER estimators and let $\varepsilon \geq 0$. If $\Delta_X(\widehat{R}) + \delta_n(\widehat{R}) \geq -\varepsilon$, for all $\widehat{R} \in \mathcal{R}_X$, then $\mathcal{G}_{X,n}^{\min}(\mathcal{R}_X) \leq \varepsilon$.*

Throughout the experimental section we observe that both the bias and the n -sampled distance from the asymptotic regime, i.e. slowness of convergence rates, are still too significant, in which case one can take $\varepsilon = 0$. In the future, when more pre-trained embeddings become available, one could expect a gap to arise between taking the minimum and the optimal estimator. However, for 1NN estimators one has guarantee that $\varepsilon = \frac{1}{2}R_X^*$ is always valid, which makes a favorable trade-off with respect to the reduced bias that good estimators will bring. We provide the proof of Lemma 3.1, and further discussions, in Section A of the supplementary material.

3.3 Efficient Implementation

As we will show in the next section, a powerful family of estimators that often outperforms others relies on the 1NN classifier evaluated on *pre-trained* feature transformations available online. This is the default setting of ease.ml/snoopy. We now present optimizations that improve the performance of this specific setting.

Algorithm. There are five computational steps involved:

- (i) Take user's dataset with n samples: features X_1, X_2, \dots, X_n and labels Y_1, Y_2, \dots, Y_n .
- (ii) For pre-defined m transformations $\mathcal{F} = \{f_1, f_2, \dots, f_m\}$, calculate the corresponding features for every sample in the dataset by applying all the transformations in \mathcal{F} .
- (iii) For each feature transformation $j \in [m]$, calculate the 1NN classifier error R_j on the transformed features $f_j(X_i)$, for all samples $i \in [n]$ and the original labels.
- (iv) Based on the 1NN classifier error, derive the lower-bound estimate for each transformation \widehat{R}_j by applying Equation 4.
- (v) Report the overall estimate by taking $\min \widehat{S}_X = \min_{j \in [m]} \widehat{R}_j$.

Note that the dataset can be split into training samples and test samples if required. The test set is only used to estimate the accuracy of the classifier and is typically orders of magnitude smaller than the training set. The quality of ease.ml/snoopy depends heavily on the list of feature transformations that are fed into it. Since we take the minimum over all transformations in \mathcal{F} , increasing the size of the set only *improves* the estimator. On the downside, an efficient implementation of such a system is by no means trivial with an ever-increasing number of (publicly) available transformations.

Computational Bottleneck. When analyzing the previously defined algorithm, we realize that the major computational bottleneck comes from transforming the features. Especially when having large pre-trained networks as feature extractors, running inference on large datasets, in order to get the embeddings, can be very time-consuming and result in running times orders of magnitude larger than the sole computation of the 1NN classifier accuracy.

Multi-armed Bandit Approach. Inspired by ideas for efficient implementations of the nearest-neighbor search on hardware accelerators [16], running inference on all the training data for all feature transformations simultaneously is not necessary. Rather, we define a streamed version of our algorithm by splitting the steps (ii) to (iv) into iterations of fixed batch size per transformation. This new formulation can directly be mapped to a *non-stochastic best arm identification* problem, where each arm represents a transformation. The successive-halving algorithm [15], which is invoked as a subroutine inside the popular Hyperband algorithm [19], is designed to solve this problem efficiently. We develop a variant of successive-halving that further improves the performance (see Section C of the supplementary material). The main idea comes from observing the *convergence curve* of a kNN classifier. We know that under some mild assumptions, the convergence curve is decreasing and convex [34]. This allows us to predict a simple lower bound for the convergence curve at the end of each step, by using an approximation of the tangent through the curve in the last point.

Efficient Incremental Execution. For the specific scenario of incrementally cleaning labels until a target accuracy is reachable, we provide a simple yet effective optimization that enables re-running ease.ml/snoopy almost instantly. After its initial execution, the system keeps track of the label of a single sample per test point – its nearest neighbor. As cleaning labels of test or training samples does not change the nearest neighbor, calculating the 1NN accuracy after cleaning an arbitrary number of training or test samples can be performed by iterating over the test set exactly once, thus, providing real-time feedback.

4 DESIGN SPACE EXPLORATION

A key design decision is determining the pool of BER estimators to use. We perform a thorough analysis of the state-of-the-art (SOTA) approaches for BER estimators described in Section 3.1. Besides having the obvious requirement of returning an *informative* estimate of the Bayes error, which in our context amounts to having a tight lower bound, the chosen estimators should also be *practical*. From a system's perspective this means scalability with respect to the number of samples and size of representations in real-world datasets, while also being insensitive to unknown hyper-parameters.

We define and illustrate the evaluation framework in Section D.1 of the supplementary material, and report the full design space exploration results in Section D.2.

Challenges and Ideas. Evaluating different BER estimators on realistic datasets is already a non-trivial task – an estimator that *underestimates* the Bayes error (e.g., by returning zero as an estimation independent of the input) will always provide a correct lower bound for the Bayes error, but will exhibit, what we call, *non-informative behavior*. Most, if not all, previous work on BER estimation avoids this issue by using synthetic datasets with *known* Bayes errors [8, 11, 35]. In order to test our estimator on real-world, high-dimensional datasets, we develop a novel methodology for evaluating BER estimators. Instead of evaluating at a single point and suffering from not knowing the ground-truth Bayes error, we propose an evaluation on a series of points, for which we know the *relative relationship* among their Bayes errors. To this end, we inject a known amount of label noise into existing datasets and follow the evolution of the Bayes error with respect to the increasing levels of noise. We can measure to which degree an estimator under-/over-estimates the Bayes error based the two quantities $u_{\mathcal{D}}(\rho)$ (a valid upper bound on the BER based on the state-of-the-art of \mathcal{D}) and $\ell_{\mathcal{D}}(\rho)$ (a valid lower bound), both derived theoretically from varying the amount of noise ρ . We combine the under-/over-estimated regions into the *BER estimator score* $E_{\mathcal{D},m}$ used for comparing different BER estimators, with $E_{\mathcal{D},m} \in [0, \frac{C+1}{2C}]$; and the lower the value is, the better the estimator is.

4.1 Summary of Results

The major findings of the empirical design space exploration lead to the conclusion that only 1NN on raw and transformed features manages to surpass the key challenges of being (1) computational feasible, and (2) insensitive to different hyper-parameters. Therefore, 1NN is our default choice for `ease.ml/snoopy` and we now present the insights that lead to this conclusion.

Unsuccessful Hyper-parameter Selection. The indicator for the success or failure of choosing the optimal hyper-parameters is given by the variance between the different quantities when varying the minimization target. In Section D.2 of the supplementary material, we provide a detailed analysis about the impact of hyper-parameters on the different error quantities originating from the novel evaluation framework. We observe that the DE-kNN, KDE, and 1NN-kNN estimators all suffer from large variances across different sets of hyper-parameters and result in the previously described *non-informative behavior*. In conclusion, selecting the best hyper-parameters without prior knowledge of the underlying probability distribution, or the amount of label noise therein, is not feasible, as illustrated in Figure 7 of the supplementary material.

Successful Hyper-parameter Selection. Our experimental evaluation shows that neither GHP (which has no hyper-parameters), nor kNN or kNN-LOO suffers from this *non-informative behavior*. As for our last method, kNN-Extrapolation, we empirically observed that extrapolating the kNN error for various sizes of training samples leads to a zero Bayes error estimate even under large amount of label noise, which again is *non-informative* despite not having any

hyper-parameters to tune. This finding is supported by the theoretical argument of Theorem 3 in Snapp et al. [34], where the number of training samples needed to extrapolate the final estimate with high confidence is exponential in the input dimension. Therefore, we omit the evaluation of this method in the experimental section. Finally, our experimental results suggest that using $k > 1$ for both kNN and kNN-LOO can lead to a lower Bayes error estimate compared to $k = 1$. As mentioned in Section 2, missing tight bounds of type similar to Equation 2 for the multiclass problem and $k > 1$, might lead to an estimate that is further away from the optimal value than the one with $k = 1$. If tight bounds become available in the future, the system could also be extended to use kNN for $k > 1$, providing an interesting research direction in the future. Finally, we observe that GHP, one of the latest proposed estimators, yields promising results that are consistent to the 1NN or 1NN-LOO estimator (c.f., Table 8). However, due to the computational requirement of computing the minimum spanning tree for GHP and the fully connected 1NN graph for 1NN-LOO, and the fact that 1NN constantly outperforms or is on par with the other estimators, we leave efficient implementations of other estimators for future work and focus on a 1NN-enabled version of `ease.ml/snoopy` in our experiments.

5 EXPERIMENTAL EVALUATION

Having restricted the set of *successful* and *practical* Bayes error estimators, we now report the results of our empirical evaluation. We start by describing the benefits of performing a feasibility study in general, and using the binary output of `ease.ml/snoopy` over other baselines, in a very specific scenario, as motivated in the introduction. We then analyze the generalization properties of our system on certain vision tasks and conclude this section by performing a detailed accuracy and performance analysis of `ease.ml/snoopy`.

Datasets. We perform the evaluation on two data modalities that are ubiquitous in modern machine learning. The first group consists of visual classification tasks, including CIFAR10/CIFAR100, and MNIST. The second group consists of standard text classification tasks, where we focus on IMDB, SST2, and YELP. Details about the datasets are given in Section E.1 of the supplementary material.

Feature Transformations. We compile a wide range of different feature transformations including state-of-the-art pre-trained embeddings for both data modalities. The pre-trained feature transformations come from public sources such as TensorFlow Hub, PyTorch Hub, and HuggingFace Transformers (see Section E.2 of the supplementary material for further justifications and a list of all transformations).

5.1 End-To-End Use Case

We simulate a specific end-to-end use case of a feasibility study in which the user’s task contains a target accuracy and a representative dataset with a fixed fraction of noisy labels. The three actions the user can perform are: (1) clean a portion of the labels, (2) train a high accuracy model using AutoML, (3) perform a feasibility study.

Different User Interaction Models. We differentiate two main scenarios in our end-to-end experimental evaluation: (1) *without feasibility study* and (2) *with feasibility study*. Without a feasibility study,

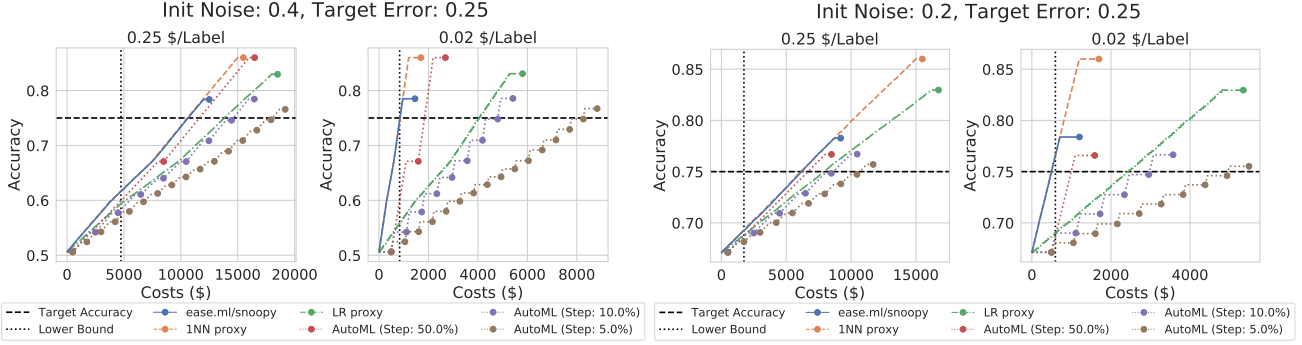


Figure 2: End-to-end use case results on CIFAR100. The plots highlight cases where using `ease.ml/snoopy` (in blue) yield the largest gain in terms of costs compared to not using any feasibility study, i.e., running only AutoML (dotted lines), or running proxy tasks 1NN (dashed orange) and logistic regression (LR) proxy model (dashed green). More results and graphs are given in the supplementary material. The end dots represent trained models accuracies after running AutoML.

users will start an initial AutoML run using the input data. If the best accuracy is below the desired target, users will clean a fixed portion of the data (1%, 5%, 10%, or 50%, which we call *steps*) and re-run the AutoML system. This is repeated until a model reaches the desired accuracy or all labels are cleaned. With a feasibility study, users alternate between running the feasibility study system and cleaning a portion of the data until the feasibility study returns a positive signal, or all labels are cleaned. Finally, a single AutoML run is performed. The lower bound on computation is given by running AutoML exactly once.

Different Estimators. We compare three different ways of conducting a feasibility study. As our baseline approaches, we train cheap models – a logistic regression (LR) model and a 1NN classifier – over all defined feature transformations and use the maximal accuracy directly as proxy. We compare these two baselines with `ease.ml/snoopy`.

Metrics. There are two factors influencing the total costs of the end-to-end use case independently of the interaction model: human labeling and computational costs. In order to balance both factors, we vary the labeling costs for realistic values and fix the machine costs to 0.9\$ per hour (the current cost of a single GPU Amazon EC2 instance).

Key Findings. The benefits of running a feasibility study using `ease.ml/snoopy` over the baselines consist of the initial label noise, the target accuracy, and the costs for cleaning labels accurately. Figure 2 illustrates the cost and accuracy for CIFAR100 and a fixed target accuracy. Each dot represents the result of one run of an AutoML system. We next summarize the key findings (I-IV), whereas additional results and the full experimental details, such as specifications of the lightweight AutoML system, the hyper-parameters used for training the LR models, and run-time of each approach, are given in Section E.3 of the supplementary material.

(I) Feasibility Study Helps. When comparing the costs of repetitively running an AutoML system to those of using an efficient and accurate system that performs a feasibility study, such as `ease.ml/snoopy`, we see significant improvements across all results (c.f., blue vs. brown lines in Figure 2). Without a system that

performs a feasibility study, users are facing a dilemma. On the one hand, if one does not run an AutoML system frequently enough, it might clean up more labels than necessary to achieve the target accuracy, e.g., AutoML (step 50%). On the other hand, if one runs an AutoML system too frequently, it is computationally expensive and one ends up wasting a lot of computation time. With a feasibility study, the user can balance these two factors better. As running low-cost proxy models is significantly cheaper than running AutoML, the user can get feedback more frequently. As seen in Figure 2, this can lead to savings in terms of costs up to a factor of 5 \times .

(II) `ease.ml/snoopy` Outperforms Baselines. When comparing different estimators that can be used in a feasibility study, in most cases, `ease.ml/snoopy` is more effective compared to running a cheaper model such as 1NN or LR with accuracy as a proxy. `ease.ml/snoopy` offers significant savings compared to 1NN when the labeling costs are high (c.f., Figure 2). The 1NN classifier will often be of a lower accuracy than an AutoML approach; hence, it requires to clean more labels than necessary to reach the target. The same holds for LR, which is significantly more expensive to run compared with `ease.ml/snoopy` and 1NN.

We note that there are cases (e.g., for IMDB) where the best LR model yields a lower error than the BER estimator used by `ease.ml/snoopy`. In such cases, there exists a regime where the costs of using the LR proxy are comparable or superior to using `ease.ml/snoopy` (c.f., Figure 10, higher labeling costs) despite being more expensive to compute. However, Figure 2 (and Figures 8, 9, 10) clearly show that the LR proxy is usually significantly more costly than using `ease.ml/snoopy`. We elaborate on the computational aspect and comparison between the `ease.ml/snoopy` and the LR proxy in Section E.3 of the supplementary material.

5.2 Generalization to Other Tasks

A potential limitation of `ease.ml/snoopy` is its dependence on having good pre-trained feature transformations for the new task. However, in practice, we observe that such good transformations often exist and we believe that more will become available in the

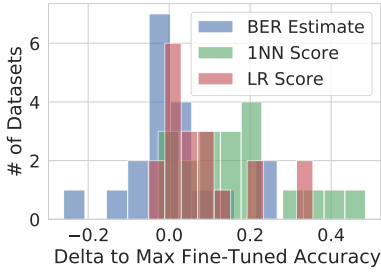


Figure 3: VTAB results based on [30].

future. To validate this, in Figure 3 we illustrate the difference between the feasibility study strategies and the best achieved post-fine-tune accuracies on the popular visual task adaptation benchmark (VTAB) [42], capturing 19 different tasks. Unsurprisingly, both LR and 1NN scores are overestimating the best possible accuracies on those tasks (except for some negative transfer results) visible in the illustrations where the values lie mainly in the positive range. In contrast, most of the datasets suggest a better or at least on par accuracy compared to only fine-tuning with 1K training samples.

5.3 Efficiency of ease.ml/snoopy

We saw that the gain of using ease.ml/snoopy comes from having an efficient estimator of high accuracy. Those two requirements are naturally connected. While having access to more and “better” (pre-trained) transformations is key for getting a high accuracy of our estimator, as analyzed in Section E.4 of the supplementary material, it requires the implementation of our algorithm to scale with respect to the ever-increasing number of transformations.

Runtime Analysis. In Figure 4 we compare different strategies for deploying the 1NN estimator on the two most complex datasets considered in this work. The strategies are evaluated with respect to the runtime (averaged across multiple independent runs on a single Nvidia Titan Xp GPU) needed to reach an estimation within 1% of the *best* possible value using all the training samples. Running the estimator only on the transformation yielding the minimal result is referred to as the *perfect* strategy providing a lower bound. We run the *successive-halving* (SH) algorithm (with and without the *tangent method* presented in Section 3.3), together with the uniform allocation baseline described in [15]. We report the runtime by selecting the best batch size out of 1%, 2%, or 5% of the training samples. Running the entire feasibility study on CIFAR100 on a single GPU takes slightly more than 16 minutes, whereas the largest examined NLP dataset YELP needs almost 8.5 hours. Putting these numbers into context, fine-tuning EfficientNet-B4 on CIFAR100 on the same GPU with one set of hyper-parameters (out of the 56 suggested by the authors [37]) requires almost 10 hours (without knowing whether other embeddings would perform better), whereas training large NLP models such as BERT is usually only achievable in a reasonable time with several hundred accelerators [26].

5.4 Discussions

BER Estimation vs. SOTA. We observe that for some datasets the estimate follows the state-of-the-art error evolution and provides a comparable value (e.g., YELP around 28%) whilst being significantly faster without training any expensive neural models or running

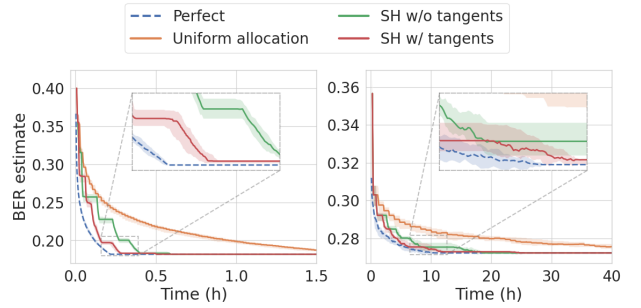


Figure 4: Different selection strategies over all transformations (Left) for CIFAR100, (Right) for YELP.

hyper-parameter searches for LR models over all transformations. This illustrates the benefit of performing a feasibility study — even though we do not directly provide the SOTA model, we provide a cheap way of producing a sensible opinion on what any model can achieve. At the same time, the estimation on some datasets can be significantly above the current SOTA (e.g., SST2 by 10.2%, or CIFAR100 by 11.7%). We believe that this is mainly due to the fact that we are currently missing diversity of transformations pre-trained on different datasets with respect to their granularity and resolution. However, in this case, a user would be presented with convergence curves (such as Figures 11 – 13 in Section E.4 of the supplementary material), as part of the insights into the system’s decision, which clearly indicates that the curves did not converge, suggesting that more data points are needed for a decisive answer.

Is Taking the Minimum Necessary? When analyzing the performance of the system with respect of the number of feature transformations, one might ask the question whether a single transformation always outperforms the others and hence makes the selection of the minimal estimator obsolete. When conducting our experiments, we see that selecting the *wrong* embedding can lead towards a large gap when compared to the optimal embedding, e.g., favoring the embedding USELARGE over XLNET on IMDB doubles the BER estimator score, $E_{\mathcal{D},m}$, whereas favoring XLNET over USELARGE on SST2 increases $E_{\mathcal{D},m}$ by 1.5×, making proper selection necessary.

6 CONCLUSION

We present ease.ml/snoopy, a novel system that provides the functionality of performing an automatic feasibility study for ML application development. By consulting a range of estimators of the Bayes error and aggregating them in a theoretically justified way, ease.ml/snoopy suggests whether a predefined target accuracy is achievable. We provide a novel evaluation framework to show the improvements over previous work on real-world datasets, and demonstrate system optimizations that support the usability of ease.ml/snoopy, which should follow the increase in the number and diversity of available pre-trained embeddings in the future.

REFERENCES

- [1] Denis Baylor, Eric Breck, Heng-Tze Cheng, Noah Fiedel, Chuan Yu Foo, Zakaria Haque, Salem Haykal, Mustafa Ispir, Vihan Jain, Levent Koc, et al. 2017. Tfx: A tensorflow-based production-scale machine learning platform. In *Proceedings of the 23rd ACM SIGKDD International Conference on Knowledge Discovery and Data Mining*. 1387–1395.
- [2] James Bergstra, Dan Yamins, and David D Cox. 2013. Hyperopt: A python library for optimizing the hyperparameters of machine learning algorithms. In *Proceedings of the 12th Python in Science Conference*, Vol. 13. Citeseer, 20.
- [3] Visar Berisha, Alan Wisler, Alfred O Hero, and Andreas Spanias. 2016. Empirically Estimable Classification Bounds Based on a Nonparametric Divergence Measure. *IEEE Transactions on Signal Processing* 64, 3 (2016), 580–591.
- [4] L J Buturovic and M Z Markovic. 1992. Improving k-nearest neighbor Bayes error estimates. In *Proceedings., 11th IAPR International Conference on Pattern Recognition. Vol.II. Conference B: Pattern Recognition Methodology and Systems*. 470–473.
- [5] Adam Byerly, Tatiana Kalganova, and Ian Dear. 2020. A Branching and Merging Convolutional Network with Homogeneous Filter Capsules. *arXiv preprint arXiv:2001.09136* (2020).
- [6] Alessandro Checco, Jo Bates, and Gianluca Demartini. 2018. All that glitters is gold—an attack scheme on gold questions in crowdsourcing. In *Proceedings of the AAAI Conference on Human Computation and Crowdsourcing*, Vol. 6.
- [7] D’Lane Compton, Tony P Love, and Jane Sell. 2012. Developing and assessing intercoder reliability in studies of group interaction. *Sociological Methodology* 42, 1 (2012), 348–364.
- [8] Thomas M. Cover and Peter A. Hart. 1967. Nearest neighbor pattern classification. *IEEE Transactions on Information Theory* 13, 1 (1967), 21–27.
- [9] Pierre A. Devijver. 1985. A multiclass, k-NN approach to Bayes risk estimation. *Pattern recognition letters* 3, 1 (1985), 1–6.
- [10] K Fukunaga and L Hostettler. 1975. k-nearest-neighbor Bayes-risk estimation. *IEEE Transactions on Information Theory* 21, 3 (1975), 285–293.
- [11] K Fukunaga and D M Hummels. 1987. Bayes Error Estimation Using Parzen and k-NN Procedures. *IEEE Transactions on Pattern Analysis and Machine Intelligence* 9, 5 (May 1987), 634–643.
- [12] K Fukunaga and D Kessell. 1973. Nonparametric Bayes error estimation using unclassified samples. *IEEE Transactions on Information Theory* 19, 4 (1973), 434–440.
- [13] Ujwal Gadiraju, Ricardo Kawase, Stefan Dietze, and Gianluca Demartini. 2015. Understanding malicious behavior in crowdsourcing platforms: The case of online surveys. In *Proceedings of the 33rd Annual ACM Conference on Human Factors in Computing Systems*. 1631–1640.
- [14] Frances Ann Hubis, Wentao Wu, and Ce Zhang. 2019. Quantitative Overfitting Management for Human-in-the-loop ML Application Development with ease.ml/meter. *arXiv preprint arXiv:1906.00299* (2019).
- [15] Kevin Jamieson and Ameet Talwalkar. 2016. Non-stochastic best arm identification and hyperparameter optimization. In *Artificial Intelligence and Statistics*. 240–248.
- [16] Jeff Johnson, Matthijs Douze, and Hervé Jégou. 2019. Billion-scale similarity search with GPUs. *IEEE Transactions on Big Data* (2019).
- [17] Alexander Kolesnikov, Lucas Beyer, Xiaohua Zhai, Joan Puigcerver, Jessica Yung, Sylvain Gelly, and Neil Houlsby. 2019. Large Scale Learning of General Visual Representations for Transfer. *arXiv preprint arXiv:1912.11370* (2019).
- [18] Tim Kraska. 2018. Northstar: An Interactive Data Science System. *PVLDB* 11, 12 (2018), 2150–2164.
- [19] Lisha Li, Kevin Jamieson, Giulia DeSalvo, Afshin Rostamizadeh, and Ameet Talwalkar. 2017. Hyperband: A novel bandit-based approach to hyperparameter optimization. *The Journal of Machine Learning Research* 18, 1 (2017), 6765–6816.
- [20] Mu Li, David G. Andersen, Jun Woo Park, Alexander J. Smola, Amr Ahmed, Vanja Josifovski, James Long, Eugene J. Shekita, and Bor-Yiing Su. 2014. Scaling Distributed Machine Learning with the Parameter Server. In *OSDI*. 583–598.
- [21] Xiangrui Meng, Joseph K. Bradley, Burak Yavuz, Evan R. Sparks, Shivaram Venkataraman, Davies Liu, Jeremy Freeman, D. B. Tsai, Manish Amde, Sean Owen, Doris Xin, Reynold Xin, Michael J. Franklin, Reza Zadeh, Matei Zaharia, and Ameet Talwalkar. 2016. MLlib: Machine Learning in Apache Spark. *Journal of Machine Learning Research* 17 (2016), 34:1–34:7.
- [22] Supun Nakandala, Arun Kumar, and Yannis Papakonstantinou. 2019. Incremental and approximate inference for faster occlusion-based deep cnn explanations. In *Proceedings of the 2019 International Conference on Management of Data*. 1589–1606.
- [23] Supun Nakandala, Yuhao Zhang, and Arun Kumar. 2020. Cerebro: a data system for optimized deep learning model selection. *Proceedings of the VLDB Endowment* 13, 12 (2020), 2159–2173.
- [24] T Pham-Gia, N Turkkan, and A Bekker. 2007. Bounds for the Bayes Error in Classification: A Bayesian Approach Using Discriminant Analysis. *Statistical Methods & Applications* 16, 1 (June 2007), 7–26.
- [25] Neoklis Polyzotis, Martin Zinkevich, Sudip Roy, Eric Breck, and Steven Whang. 2019. Data validation for machine learning. *Proceedings of Machine Learning and Systems* 1 (2019).
- [26] Jeff Rasley, Samyam Rajbhandari, Olatunji Ruwase, and Yuxiong He. 2020. DeepSpeed: System Optimizations Enable Training Deep Learning Models with Over 100 Billion Parameters. In *Proceedings of the 26th ACM SIGKDD International Conference on Knowledge Discovery & Data Mining*. 3505–3506.
- [27] Alexander Ratner, Stephen H Bach, Henry Ehrenberg, Jason Fries, Sen Wu, and Christopher Ré. 2017. Snorkel: Rapid training data creation with weak supervision. *Proceedings of the VLDB Endowment* 11, 3 (2017).
- [28] Cédric Renggli, Bojan Karlas, Bolin Ding, Feng Liu, Kevin Schawinski, Wentao Wu, and Ce Zhang. 2019. Continuous Integration of Machine Learning Models with ease.ml/ci: Towards a Rigorous Yet Practical Treatment. In *SysML Conference*.
- [29] Cedric Renggli, André Susano Pinto, Luka Rimanic, Joan Puigcerver, Carlos Riquelme, Ce Zhang, and Mario Lucic. 2020. Which Model to Transfer? Finding the Needle in the Growing Haystack. *arXiv preprint arXiv:202010.06402* (2020).
- [30] Cedric Renggli, André Susano Pinto, Luka Rimanic, Joan Puigcerver, Carlos Riquelme, Ce Zhang, and Mario Lucic. 2020. Which Model to Transfer? Finding the Needle in the Growing Haystack. *arXiv preprint arXiv:2010.06402* (2020).
- [31] Cedric Renggli, Luka Rimanic, Luka Kolar, Wentao Wu, and Ce Zhang. 2020. Ease.ml/snoopy in Action: Towards Automatic Feasibility Analysis for Machine Learning Application Development. *Proceedings of the VLDB Endowment* 13, 12 (2020).
- [32] Luka Rimanic, Cedric Renggli, Bo Li, and Ce Zhang. 2020. On Convergence of Nearest Neighbor Classifiers over Feature Transformations. *arXiv preprint arXiv:2010.07765* (2020).
- [33] Salimeh Yasaei Sekeh, Brandon Lee Oselio, and Alfred O Hero. 2020. Learning to bound the multi-class Bayes error. *IEEE Transactions on Signal Processing* (2020).
- [34] Robert R Snapp, Demetri Psaltis, and Santosh S Venkatesh. 1991. Asymptotic slowing down of the nearest-neighbor classifier. In *Advances in Neural Information Processing Systems*. 932–938.
- [35] Robert R Snapp and Tong Xu. 1996. Estimating the Bayes risk from sample data. In *Advances in Neural Information Processing Systems*. 232–238.
- [36] David Q Sun, Hadas Kotek, Christopher Klein, Mayank Gupta, William Li, and Jason D Williams. 2020. Improving Human-Labeled Data through Dynamic Automatic Conflict Resolution. *arXiv preprint arXiv:2012.04169* (2020).
- [37] Mingxing Tan and Quoc Le. 2019. EfficientNet: Rethinking model scaling for convolutional neural networks. In *International Conference on Machine Learning*. PMLR, 6105–6114.
- [38] Hans Van Vliet, Hans Van Vliet, and JC Van Vliet. 2008. *Software engineering: principles and practice*. Vol. 13. John Wiley & Sons.
- [39] Manasi Vartak, Harihar Subramanyam, Wei-En Lee, Srinidhi Viswanathan, Saadiyah Husnoo, Samuel Madden, and Matei Zaharia. 2016. ModelDB: a system for machine learning model management. In *Proceedings of the Workshop on Human-In-the-Loop Data Analytics*. 1–3.
- [40] Zhilin Yang, Zihang Dai, Yiming Yang, Jaime Carbonell, Russ R Salakhutdinov, and Quoc V Le. 2019. Xlnet: Generalized autoregressive pretraining for language understanding. In *Advances in Neural Information Processing Systems*. 5754–5764.
- [41] Matei Zaharia, Andrew Chen, Aaron Davidson, Ali Ghodsi, Sue Ann Hong, Andy Konwinski, Siddharth Murching, Tomas Nykodym, Paul Ogilvie, Mani Parkhe, et al. 2018. Accelerating the Machine Learning Lifecycle with MLflow. *IEEE Data Eng. Bull.* 41, 4 (2018), 39–45.
- [42] Xiaohua Zhai, Joan Puigcerver, Alexander Kolesnikov, Pierre Ruysen, Carlos Riquelme, Mario Lucic, Josip Djolonga, Andre Susano Pinto, Maxim Neumann, Alexey Dosovitskiy, et al. 2019. A large-scale study of representation learning with the visual task adaptation benchmark. *arXiv preprint arXiv:1910.04867* (2019).

A TAKING THE MINIMUM OVER ALL ESTIMATORS

In this section we provide proof and a discussion for the theoretical claim presented in the main body that is not part of our theoretical companion to this paper [32].

PROOF OF LEMMA 3.1: Let

$$\mathcal{R}_n^+ := \left\{ \widehat{R} \in \mathcal{R}_X : R_X^* \geq \widehat{R}_n \right\}, \quad \mathcal{R}_n^- := \left\{ \widehat{R} \in \mathcal{R}_X : R_X^* < \widehat{R}_n \right\}.$$

We have

$$\begin{aligned} \min_{\widehat{R} \in \mathcal{R}_X} \mathcal{G}_{X,n}(\widehat{R}) &= \min \left\{ \min_{\widehat{R} \in \mathcal{R}_n^+} (R_X^* - \widehat{R}_n), \min_{\widehat{R} \in \mathcal{R}_n^-} (\widehat{R}_n - R_X^*) \right\} \\ &= \min \left\{ R_X^* - \max_{\widehat{R} \in \mathcal{R}_n^+} \widehat{R}_n, -R_X^* + \min_{\widehat{R} \in \mathcal{R}_n^-} \widehat{R}_n \right\}, \end{aligned}$$

implying that

$$\arg \min_{\widehat{R} \in \mathcal{R}_n^-} \mathcal{G}_{X,n}(\widehat{R}) = \arg \min_{\widehat{R} \in \mathcal{R}_n^-} \widehat{R}_n. \quad (5)$$

For all $\widehat{R} \in \mathcal{R}_n^+$ we have that

$$R_X^* - \widehat{R}_n = (R_X^* - \widehat{R}) + (\widehat{R} - \widehat{R}_n) = -\Delta_X(\widehat{R}) - \delta_n(\widehat{R}) \leq \varepsilon,$$

yielding

$$0 \leq \min_{\widehat{R} \in \mathcal{R}_n^+} \mathcal{G}_{X,n}(\widehat{R}) \leq \mathcal{G}_{X,n}(\arg \min_{\widehat{R} \in \mathcal{R}_n^+} \widehat{R}) \leq \varepsilon.$$

Combining this with Equation 5 yields the claim. \square

It is clear that the strength of estimator $\widehat{S}_X = \min_{\widehat{R} \in \mathcal{R}_X} \widehat{R}$ depends on the quality of estimators in \mathcal{R}_X . Lemma 3.1 establishes that a strategy as simple as choosing the minimum is either optimal (in case when one can take $\varepsilon = 0$) or only slightly off, with respect to the best possible estimator in \mathcal{R}_X .

Discussion. In order to fully grasp the strength of Lemma 3.1, we need to examine the validity of the assumptions. The bias reflects the quality of the estimator in the asymptotic regime, which is expected to be small for any useful estimator, even though it is only a lower bound. For example, for every $\varepsilon > 0$ there exists k_ε such that $h_{\infty, k_\varepsilon}$, the infinite-sample k_ε NN estimator, satisfies $\Delta_X(h_{\infty, k_\varepsilon}) \geq -\varepsilon$. When $k = 1$, the 1NN-based estimator from Equation 4 results in a sub-optimal ε for the bias itself. However, throughout the experimental section we observe that both the bias and the n -sampled distance from the asymptotic regime, i.e. slowness of convergence rates, are still too significant. Therefore, in practice we observe that $\varepsilon = 0$ is achievable, whereas in the future, when more pre-trained embeddings become available, $\varepsilon > 0$ will become important. In that case, it is important to note that for 1NN estimator defined in Equation 4, using the fact that $(R_X)_{n,1} \geq R_X^*$, since 1NN is a classifier, one has

$$R_X^* - \widehat{R}_n = R_X^* - \frac{(R_X)_{n,1}}{1 + \sqrt{1 - \frac{C(R_X)_{n,1}}{C-1}}} \leq R_X^* - \frac{R_X^*}{1 + \sqrt{1 - \frac{C(R_X)_{n,1}}{C-1}}} \leq \frac{1}{2} R_X^*,$$

proving that one can always take $\varepsilon = \frac{1}{2} R_X^*$.

B DESIGN SPACE: BAYES ERROR ESTIMATORS

We provide a detailed description of existing BER estimators in this section by dividing them into three groups, reflected in the following equation:

$$R_X^* = \underbrace{\mathbb{E}_X \left[\underbrace{1 - \max_{y \in \mathcal{Y}} \eta_y(x)}_{(1)} \right]}_{(3)}. \quad (6)$$

(1) *Density estimators.* Both methods in this group use the full training set with labels to estimate the class posterior, repeated once again for the same training set, but this time without the labels. This allows one to sample the feature space accordingly and get an estimate of the expectation over \mathcal{X} . **(DE-kNN)** This method estimates the per-class posterior η_y for all $y \in \mathcal{Y}$, by counting the fraction k_y/k of training samples with that specific label amongst the k -nearest-neighbors, in expectation over the feature space [12]. One uses the full training set only to estimate an upper bound by the leave-one-out (LOO) technique, and an optimistic lower bound by the re-substitution technique [11]. **(KDE)** This method estimates the class prior by first taking a fraction of per-class samples in the full training set. Using a kernel density approach, the class likelihood is then estimated using all the samples per class separately. Finally, by using the Bayes formula, one can derive the posterior density per class, which is used as lower and upper bound.

(2) *Divergence estimator.* **(GHP)** This estimator uses the generalized Henze-Penrose divergence [33] between every pair of η_i and η_j , to get a provably valid estimator of the BER in the asymptotic regime. The estimation of the divergence can be further utilized to get an upper-/lower-bound estimate of the BER. Implementation-wise, one first constructs the minimum spanning tree (MST) over the fully connected graph over all the samples, with edges being defined through Euclidean distances, and then uses the number of dichotomous edges to estimate the BER, noting that GHP and kNN-LOO have similar computational complexity. This method uses only a single set of samples.

(3) *kNN classifier accuracy.* **(1NN-kNN)** The approach by Devijver [9] aims at estimating the 1NN classifier accuracy by using the k -nearest-neighbor information. In order to get an unbiased estimator of the 1NN classifier accuracy, Devijver [9] proposed using $\frac{1}{k(k-1)} \sum_{y \in \mathcal{Y}} k_y(k - k_y)$ as the estimator, where k is the hyper-parameter of the method. This approach is very similar to *DE-kNN*, with the difference that we are not estimating η_y based on a labels training set, but directly the 1NN classifier accuracy. Training set is usually used twice through the resubstitution technique in order to get the 1NN classifier accuracy. **(kNN-LOO)** When one wants to omit splitting the dataset into test and train sets, the kNN classifier accuracy can be reported using a leave-one-out approach. In this work we simply use this estimator for a fair comparison with certain non-scalable methods, noting that this approach is typically not computationally feasible in practice. **(kNN-Extrapolation)** One major caveat of bounding the Bayes error rate by any kNN accuracy method lies in the fact that the bounds hold only in the asymptotic regime. As an attempt to surpass this limitation, Snapp and Xu [35] extrapolate the convergence values of kNN for different number of training samples by assuming probability densities with uniformly bounded partial derivatives up through order N . However, this requires the number of samples to be exponential in the input dimension and, hence, is incapable of generalizing to representations of higher dimension on real-world datasets. **(kNN)** Another simple estimator, directly inspired by Cover and Hart [8], recalling that such an expression exists for $C > 2$ only when $k = 1$, uses the validation error rate of a 1NN classifier $(R_X)_{n,1}$ after normalizing:

$$\widehat{R}_{X,h_{n,1}} := \frac{(R_X)_{n,1}}{1 + \sqrt{1 - \frac{C(R_X)_{n,1}}{C-1}}}. \quad (7)$$

C SUCCESSIVE-HALVING WITH TANGENTS

In Section 3.3 we illustrated the successive-halving algorithm together with the improvement that uses tangent predictions to avoid unnecessary calculations on transformations that will certainly not proceed to the next step. In this section we provide an illustration of the algorithm in Figure 5 along with pseudocodes for both variants of the successive-halving algorithm. Switching from one variant to the other is simply done through the `use_tangent` flag, which either calls the function `Pulls_with_tangent_breaks`, or avoids this and performs the original successive-halving algorithm. As the remaining transformations after each step are the same in both variants, all theoretical guarantees of successive-halving can be transferred to our extension.

The `Pulls_with_tangent_breaks` function simply uses the tangent, which we approximate by a line through the two last known points of the convergence curve, to predict the smallest error that a feature transformation can achieve at the end of the current step. Here we assume that the convergence curves are convex, which holds on average [34]. Therefore, it is a slightly more aggressive variant of the successive-halving algorithm, but we did not observe failures in practice since the tangent is usually a very crude lower bound.

Parameters of successive-halving. We eliminate the dependency on the initial budget by implementing the *doubling-trick* (cf. Section 3 in [15]). The batch size for the iterations has a direct impact on the performance and speedup of the algorithm when compared to other approaches. This is linked to properties of the underlying hardware and the fact that approximating the tangent for points that are further apart becomes less accurate. Hence, we treat the batch size as a single hyper-parameter.

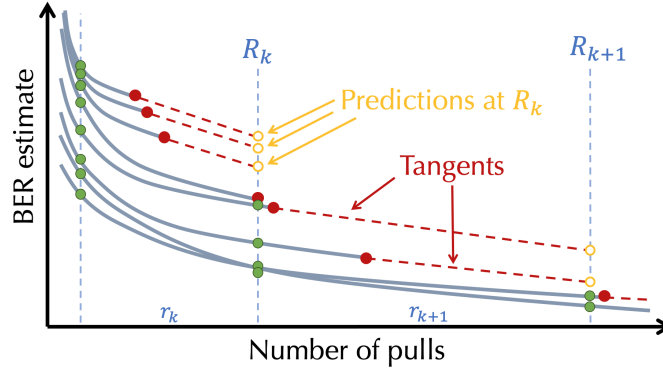


Figure 5: Illustration of the successive-halving algorithm with early elimination of candidates using tangents.

Algorithm 1 Successive-Halving with Tangents

Input: Flag use_tangent, budget B , arms $1, \dots, n$ with $l_{i,k}$ denoting the k -th loss from the i -th arm

Initialize: $S_0 = [n]$, predictions $[i] = 0$, for all $i \in [n]$

for $k = 0, 1, \dots, \lceil \log_2(n) \rceil - 1$ **do**

$L = |S_k|$;

$r_k = \lfloor \frac{B}{L \cdot \lceil \log_2(n) \rceil} \rfloor$

$R_k = \sum_{j=0}^k r_j$

 Pull r_k times each arm $i = 1, \dots, \lfloor L/2 \rfloor$

if not use_tangent **then**

 Pull r_k times each arm $i = \lfloor L/2 \rfloor + 1, \dots, L$

else

 threshold = $\max_{i=1, \dots, \lfloor L/2 \rfloor} l_{i,R_k}$

$S_k = \text{Pulls_with_tangent_breaks}(S_k, r_k, R_k, \text{predictions}[], \text{threshold})$

end if

 Let σ_k be a permutation on S_k such that $l_{\sigma_k(1), R_k} \leq \dots \leq l_{\sigma_k(|S_k|), R_k}$

$S_{k+1} = \{\sigma_k(1), \dots, \sigma_k(\lfloor L/2 \rfloor)\}$.

end for

Output: Singleton element of $S_{\lceil \log_2(n) \rceil}$

Algorithm 2 Pulls_with_tangent_breaks

Input: $S, r, R, \text{predictions}[], \text{threshold}$

for $i \in S$ **do**

for $j = 1, \dots, r$ **do**

if predictions $[i] > \text{threshold}$ **then**

 remove i from S

break

else

 Pull arm i once

 Update predictions $[i]$ using tangent value at R

end if

end for

end for

Return S

D DESIGN SPACE EXPLORATION

We present the complete design space exploration next. As outlined in the main part of this work, evaluating any BER estimate on real-world datasets without having knowledge of the underlying probability distribution is non-trivial. Especially when focusing on well-established

benchmark datasets such as MNIST or CIFAR10, one might be tempted to estimate a zero-valued BER. This approach is of course *non-informative* although probably not far from the real BER value. Benchmark datasets are typically collected (e.g., by requesting multiple labels per sample to remove noise) such that perfect classifiers are conceivable. In order to still evaluate BER estimators on such datasets we can make use of strong state-of-the-art (SOTA) results with years of incremental research, and derive a novel evaluation methodology which calculates a score by injecting different levels of controlled label noise.

D.1 Evaluation Framework

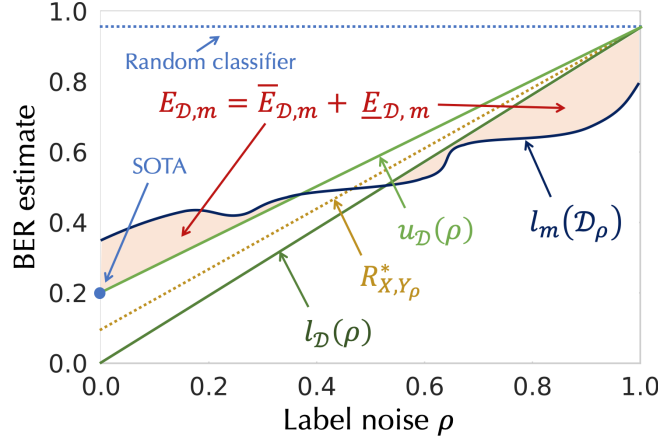


Figure 6: Evaluation Methodology

Let \mathcal{D} be a dataset containing n i.i.d. samples from $p(X, Y)$. Let $s_{\mathcal{D}}$ denote the *known state-of-the-art (SOTA) classification performance*, achieved by some classifier and, thus, an upper bound on the Bayes error R_X^* . Now assume that we assign a uniformly random label with probability $\rho \in [0, 1]$ to each sample. The following result quantifies the increase in the Bayes error introduced this way⁴.

LEMMA D.1. Let Y_{ρ} be a random variable defined on \mathcal{Y} by setting $Y_{\rho} = Z \cdot U(\mathcal{Y}) + (1 - Z) \cdot Y$, where U is a uniform variable taking values in \mathcal{Y} , and Z is a Bernoulli variable with probability $0 \leq \rho \leq 1$, both independent of X and Y . Then $R_{X,Y_{\rho}}^* = R_{X,Y}^* + \rho(1 - 1/C - R_{X,Y}^*)$.

PROOF: Let $p(X, Y_{\rho})$ be the corresponding joint distribution on $\mathcal{X} \times \mathcal{Y}$ for the random variables X and Y_{ρ} , simplified as $p_{\rho}(x, y)$. Note that

$$p_{\rho}(y|x) = \underbrace{p_{\rho}(y|x, Z=0) p(Z=0)}_{p(y|x)} + \underbrace{p_{\rho}(y|x, Z=1) p(Z=1)}_{p(U=y)} = (1 - \rho)p(y|x) + \frac{\rho}{C}.$$

Therefore,

$$R_{X,Y_{\rho}}^* = \mathbb{E}_X \left[1 - \max_{y \in \mathcal{Y}} p_{\rho}(y|x) \right] = 1 - \mathbb{E}_X \max_{y \in \mathcal{Y}} \left[(1 - \rho)p(y|x) + \frac{\rho}{C} \right] = 1 - \frac{\rho}{C} - (1 - \rho) \mathbb{E}_X \max_{y \in \mathcal{Y}} p(y|x) = R_{X,Y}^* + \rho(1 - 1/C - R_{X,Y}^*).$$

□

We remark that $Y_{\rho} \in \mathcal{Y}$, where ρ corresponds to the probability of randomly changing the original label to a random value in \mathcal{Y} ⁵.

As a direct consequence of Lemma D.1, using the SOTA as an upper bound for R_X^* , and $R_X^* \geq 0$ as the lower bound, we can define the valid bounds on $R_{X,Y_{\rho}}^*$:

$$u_{\mathcal{D}}(\rho) = s_{\mathcal{D}} + \rho(1 - 1/C - s_{\mathcal{D}}), \quad \ell_{\mathcal{D}}(\rho) = \rho(1 - 1/C),$$

yielding $R_{X,Y_{\rho}}^* \in [\ell_{\mathcal{D}}(\rho), u_{\mathcal{D}}(\rho)]$. For a fixed method m , we can estimate the lower bound $\ell_m(\mathcal{D}_{\rho})$ using any of the previously described Bayes error estimation method on a manipulated dataset \mathcal{D}_{ρ} obtained by taking $\rho \cdot n$ samples out of \mathcal{D} , and randomly changing their labels, whilst keeping the other $(1 - \rho) \cdot n$ samples intact. Notice that our evaluation framework needs to change the label on all the data points (i.e. in both the training and test sets).

⁴The statement of Lemma D.1, without a proof, appears in our short VLDB 2020 demo paper [31].

⁵Lemma D.1 implies that $1 - 1/C \geq R_{X,Y_{\rho}}^* \geq R_{X,Y}^*$.

As illustrated in Figure 6, in order to define the error of a given method m on the modified dataset \mathcal{D}_ρ , we can estimate two areas with respect to the curves: (i) *the area where m clearly underestimates the Bayes error lower bound*, and (ii) *the area where m clearly overestimates the Bayes error lower bound*. More formally, we define the BER estimator score $E_{\mathcal{D},m} := \underline{E}_{\mathcal{D},m} + \bar{E}_{\mathcal{D},m}$, where

$$\begin{aligned}\underline{E}_{\mathcal{D},m} &:= \int_{\rho=0}^1 \left(\mathbf{1}_{\{\ell_m(\mathcal{D}_\rho) < l_{\mathcal{D}}(\rho)\}} (l_{\mathcal{D}}(\rho) - \ell_m(\mathcal{D}_\rho)) \right) d\rho, \\ \bar{E}_{\mathcal{D},m} &:= \int_{\rho=0}^1 \left(\mathbf{1}_{\{\ell_m(\mathcal{D}_\rho) > u_{\mathcal{D}}(\rho)\}} (l_m(\mathcal{D}_\rho) - u_{\mathcal{D}}(\rho)) \right) d\rho.\end{aligned}$$

For every method m it holds that $\mathbb{E} [E_{\mathcal{D},m}] \in [0, \frac{C+1}{2C}]$. It is equal to zero if and only if for all $\rho \in [0, 1]$, we have $\mathbb{E} [\ell_m(\mathcal{D}_\rho)] \in [\ell_{\mathcal{D}}(\rho), u_{\mathcal{D}}(\rho)]$, in which case the method m is an *optimal* lower-bound estimate. Consequently, for two methods m and m' , $\mathbb{E} [E_{\mathcal{D},m}] < \mathbb{E} [E_{\mathcal{D},m'}]$ implies that m yields a *better* estimate compared to m' , in expectation.

We will use $E_{\mathcal{D},m}$ to assess the performance of existing methods and our proposed estimator. We estimate the expectation and standard deviation of the score $S_{\mathcal{D},m}$ by sampling linearly 10 values for ρ and constructing 30 random datasets \mathcal{D}_ρ for every sampled ρ .

D.2 Evaluation of Bayes Error Estimators

We summarize the results of our extensive design space exploration by describing the major challenges encountered when defining the set of reasonable BER estimators for `ease.ml/snoopy`.

Challenge 1: Computational feasibility. We start by emphasizing that running every estimator on raw features might not be feasible in practice on large-scale datasets. There are multiple reasons for this, but the main challenges are twofold. First, we are often bound by hardware limitations (e.g., memory). This is visible at runtime, when a given method requires to store all the training (and test, if different) samples in memory for running the algorithm. In order to show the applicability of our system, we implement a streamed and batched version for kNN estimator which runs with constant memory and can make use of hardware accelerators. This allows us to run `ease.ml/snoopy` on datasets as large as ImageNet. Extending other methods to scale beyond the typical hardware limitations is beyond the scope of this paper since they are already outperformed by the kNN estimator. For example, running kNN-LOO or GHP on a large number of samples is often not feasible. For kNN-LOO this is obvious since it needs the whole square matrix of the input dataset, whereas GHP requires calculating a subgraph (MST) over the fully connected graph with pairwise distance between all the training samples.

A note on GHP vs 1NN. When looking at the derivation of both the upper and lower bounds of GHP (Theorem 1 by Sekeh et al. [33]), we see that, asymptotically, this method averages the number of dichotomous edges connecting a sample from two different classes, on the minimum spanning tree (MST) that is connecting all the samples in Euclidean space. The 1NN-LOO estimator implicitly performs the same task over the 1-nearest-neighbor graph, instead of the MST. Intuitively, the 1-nearest-neighbor graph should lead to a slightly lower error rate when compared to the MST. In particular, 1NN-LOO should outperform GHP if the feature transformation forms well-separable clusters of samples from the same class. Nevertheless, showing this is beyond the scope of this work and left for future work.

Challenge 2: Hyper-parameter selection. Given a dataset and a fixed method with one or more hyper-parameters, what criteria should be used to select the *best* hyper-parameters? As motivated before, selecting the set of parameters that minimize the BER estimate (or its lower bound) might lead to underestimating the Bayes error. Using the error $E_{\mathcal{D},m}$ introduced in Section D.1, together with the two summands $\bar{E}_{\mathcal{D},m}$ and $\underline{E}_{\mathcal{D},m}$, we see that any estimator that over-estimates the Bayes error under label noise results in a large error term $\bar{E}_{\mathcal{D},m}$. We define a meaningful range of hyper-parameters per method in Table 1 on each of the computer vision datasets from Table 5. The list was manually curated during the evaluation process by shrinking the range of possible values to get the best possible set of hyper-parameters per dataset and per method. We focus on this specific modality as we do not want to artificially increase the Bayes error by applying any transformation, but rather use the raw input features. Remember that there are no raw feature representations for text, as even simple bag-of-words can increase the Bayes error – imagine two sentences containing the same words but different orderings and different labels. Both sentences would clearly result in the same feature vector after applying the bag-of-words transformation, whereas different labels would yield an increase in the Bayes error.

Table 1: Hyper-parameters on all methods and datasets.

	DE-kNN	Gaussian KDE	kNN-LOO and kNN (cosine and L_2)	1NN-kNN
MNIST	$k \in [2, 100]$	$B \in \{0.0005, 0.001, 0.01, 0.1\}$	$k \in [1, 25]$	$k \in [2, 100]$
CIFAR10	$k \in [2, 100]$	$B \in \{0.05, 0.1, 0.2, 0.4\}$	$k \in [1, 25]$	$k \in [2, 100]$
CIFAR100	$k \in [2, 100]$	$B \in \{0.001, 0.05, 0.01, 0.2, 0.4\}$	$k \in [1, 25]$	$k \in [2, 100]$

In order to further illustrate the impracticability of setting the unknown parameters and their effect on the estimated Bayes error, we define four different quantities which are minimized in order to pick the hyper-parameters: (i) the Bayes error estimate (or its lower bound),

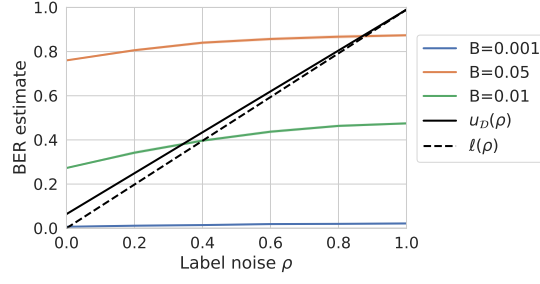


Figure 7: Gaussian KDE estimation on the raw pixel input for CIFAR100 and varying hyper-parameters. Notice that all the curves either clearly under- or over-estimate the Bayes error for a fixed percentage of label noise that makes the choice of *optimal* hyper-parameters infeasible and the estimator *non-informative*.

(ii) $\bar{E}_{\mathcal{D},m}$ – the area where we overestimate the Bayes error, (iii) $\underline{E}_{\mathcal{D},m}$ – the area where we underestimate the Bayes error, and (iv) $E_{\mathcal{D},m}$ – sum of areas in (ii) and (iii). The best hyper-parameters chosen independently of the quantity that is minimized should not significantly increase other values. We report the resulting values and picked hyper-parameters for the three vision datasets in Tables 2, 3 and 4.

Unsuccessful hyper-parameter selection. As described in the main body of the paper, we observe that selecting the optimal hyper-parameters for the methods DE-kNN, Gaussian KDE and 1NN-kNN is not feasible. Minimizing any of the four previously described quantities results in a large variation of scores for other quantities. Additionally, all three methods are largely underestimating the Bayes error when increasing the label noise, which is visible in the value reported for $\underline{E}_{\mathcal{D},m}$, except when minimizing this value, where the resulting BER estimation for zero label noise increases drastically. This is precisely the *non-informative* behavior described in the paper and illustrated in Figure 7.

Successful hyper-parameter selection. The above behavior is not observed when analyzing kNN, kNN-LOO and GHP, where $\underline{E}_{\mathcal{D},m}$ is constantly zero except for the first two rows in Table 2, where minimizing the Bayes error estimate for kNN and kNN-LOO picks a hyper-parameter $k > 1$. The reason for having a positive error below the trivial lower bound is the lack of tight-bound derivations for multi-class kNN Bayes error estimation using $k > 1$, as outlined multiple times in the main body. This further motivates the use of 1NN (i.e. kNN with $k = 1$) as the choice of our default algorithm, which we highlight in bold in all the tables that show the results for the hyper-parameter selection.

Table 2: Full results on *raw* input features of MNIST.

	DE-kNN	Gaussian KDE	kNN-LOO	kNN	1NN	1NN-kNN	GHP
Parameters	k=2	B=0.0005	k=3 (cosine)	k=4 (cosine)	k=1 (cosine)	k=2	-
min BER	2%	36%	2%	1%	1%	1%	3%
$\bar{E}_{\mathcal{D},m}$	0% ($\pm 0.02\%$)	18% ($\pm 2.23\%$)	0% ($\pm 0.07\%$)	0% ($\pm 0.03\%$)	1% ($\pm 0.38\%$)	0% ($\pm 0.00\%$)	1% ($\pm 0.44\%$)
$\underline{E}_{\mathcal{D},m}$	15% ($\pm 0.17\%$)	6% ($\pm 1.60\%$)	3% ($\pm 0.66\%$)	5% ($\pm 0.54\%$)	0% ($\pm 0.32\%$)	28% ($\pm 0.12\%$)	0% ($\pm 0.34\%$)
$E_{\mathcal{D},m}$	16% ($\pm 0.18\%$)	24% ($\pm 3.60\%$)	3% ($\pm 0.64\%$)	5% ($\pm 0.53\%$)	1% ($\pm 0.57\%$)	28% ($\pm 0.12\%$)	2% ($\pm 0.65\%$)
Parameters	k=2	B=0.0005	k=6 (cosine)	k=8 (cosine)	k=1 (cosine)	k=2	-
BER	2%	36%	2%	1%	1%	1%	3%
min $\bar{E}_{\mathcal{D},m}$	0% ($\pm 0.02\%$)	18% ($\pm 2.23\%$)	0% ($\pm 0.00\%$)	0% ($\pm 0.00\%$)	1% ($\pm 0.38\%$)	0% ($\pm 0.00\%$)	1% ($\pm 0.44\%$)
$\underline{E}_{\mathcal{D},m}$	15% ($\pm 0.17\%$)	6% ($\pm 1.60\%$)	7% ($\pm 0.58\%$)	8% ($\pm 0.45\%$)	0% ($\pm 0.32\%$)	28% ($\pm 0.12\%$)	0% ($\pm 0.34\%$)
$E_{\mathcal{D},m}$	16% ($\pm 0.18\%$)	24% ($\pm 3.60\%$)	7% ($\pm 0.58\%$)	8% ($\pm 0.45\%$)	1% ($\pm 0.57\%$)	28% ($\pm 0.12\%$)	2% ($\pm 0.65\%$)
Parameters	k=100	B=0.1	k=1 (L_2)	k=1 (cosine)	k=1 (cosine)	k=99	-
BER	19%	70%	2%	1%	1%	15%	3%
$\bar{E}_{\mathcal{D},m}$	9% ($\pm 0.20\%$)	36% ($\pm 0.57\%$)	1% ($\pm 0.53\%$)	1% ($\pm 0.38\%$)	1% ($\pm 0.38\%$)	7% ($\pm 0.24\%$)	1% ($\pm 0.44\%$)
min $\underline{E}_{\mathcal{D},m}$	0% ($\pm 0.01\%$)	1% ($\pm 0.11\%$)	0% ($\pm 0.33\%$)	0% ($\pm 0.32\%$)	0% ($\pm 0.32\%$)	0% ($\pm 0.06\%$)	0% ($\pm 0.34\%$)
$E_{\mathcal{D},m}$	10% ($\pm 0.21\%$)	37% ($\pm 0.68\%$)	1% ($\pm 0.72\%$)	1% ($\pm 0.57\%$)	1% ($\pm 0.57\%$)	7% ($\pm 0.31\%$)	2% ($\pm 0.65\%$)
Parameters	k=12	B=0.0005	k=1 (cosine)	k=1 (L_2)	k=1 (cosine)	k=19	-
BER	7%	36%	2%	1%	1%	7%	3%
$\bar{E}_{\mathcal{D},m}$	3% ($\pm 0.16\%$)	18% ($\pm 2.23\%$)	1% ($\pm 0.47\%$)	1% ($\pm 0.38\%$)	1% ($\pm 0.38\%$)	3% ($\pm 0.18\%$)	1% ($\pm 0.44\%$)
$\underline{E}_{\mathcal{D},m}$	2% ($\pm 0.06\%$)	6% ($\pm 1.60\%$)	0% ($\pm 0.34\%$)	0% ($\pm 0.32\%$)	0% ($\pm 0.32\%$)	1% ($\pm 0.08\%$)	0% ($\pm 0.34\%$)
min $E_{\mathcal{D},m}$	5% ($\pm 0.21\%$)	24% ($\pm 3.60\%$)	1% ($\pm 0.65\%$)	1% ($\pm 0.57\%$)	1% ($\pm 0.57\%$)	4% ($\pm 0.27\%$)	2% ($\pm 0.65\%$)

Table 3: Full results on *raw* input features of of CIFAR10.

	DE-kNN	Gaussian KDE	kNN-LOO	kNN	1NN	1NN-kNN	GHP
Parameters	k=2	B=0.4	k=1 (cosine)	k=1 (cosine)	k=1 (cosine)	k=2	-
min BER	36%	0%	47%	41%	41%	40%	50%
$\bar{E}_{\mathcal{D},m}$	9% ($\pm 0.07\%$)	0% ($\pm 0.00\%$)	23% ($\pm 0.92\%$)	20% ($\pm 0.78\%$)	20% ($\pm 0.78\%$)	13% ($\pm 1.71\%$)	25% ($\pm 0.91\%$)
$\underline{E}_{\mathcal{D},m}$	13% ($\pm 0.09\%$)	45% ($\pm 0.00\%$)	0% ($\pm 0.21\%$)	0% ($\pm 0.25\%$)	0% ($\pm 0.25\%$)	7% ($\pm 0.76\%$)	0% ($\pm 0.24\%$)
$\overline{E}_{\mathcal{D},m}$	22% ($\pm 0.16\%$)	45% ($\pm 0.00\%$)	23% ($\pm 1.10\%$)	20% ($\pm 1.03\%$)	20% ($\pm 1.03\%$)	20% ($\pm 2.39\%$)	25% ($\pm 1.15\%$)
Parameters	k=2	B=0.4	k=25 (cosine)	k=25 (cosine)	k=1 (cosine)	k=2	-
BER	36%	0%	48%	42%	41%	40%	50%
min $\bar{E}_{\mathcal{D},m}$	9% ($\pm 0.07\%$)	0% ($\pm 0.00\%$)	20% ($\pm 0.74\%$)	16% ($\pm 0.65\%$)	20% ($\pm 0.78\%$)	13% ($\pm 1.71\%$)	25% ($\pm 0.91\%$)
$\underline{E}_{\mathcal{D},m}$	13% ($\pm 0.09\%$)	45% ($\pm 0.00\%$)	0% ($\pm 0.23\%$)	0% ($\pm 0.24\%$)	0% ($\pm 0.25\%$)	7% ($\pm 0.76\%$)	0% ($\pm 0.24\%$)
$\overline{E}_{\mathcal{D},m}$	22% ($\pm 0.16\%$)	45% ($\pm 0.00\%$)	20% ($\pm 0.93\%$)	17% ($\pm 0.87\%$)	20% ($\pm 1.03\%$)	20% ($\pm 2.39\%$)	25% ($\pm 1.15\%$)
Parameters	k=100	B=0.2	k=5 (cosine)	k=2 (cosine)	k=1 (cosine)	k=10	raw - ghp
BER	65%	89%	48%	44%	41%	53%	50%
$\bar{E}_{\mathcal{D},m}$	31% ($\pm 0.32\%$)	44% ($\pm 0.08\%$)	22% ($\pm 0.86\%$)	22% ($\pm 0.77\%$)	20% ($\pm 0.78\%$)	32% ($\pm 0.69\%$)	25% ($\pm 0.91\%$)
min $\underline{E}_{\mathcal{D},m}$	0% ($\pm 0.01\%$)	0% ($\pm 0.02\%$)	0% ($\pm 0.15\%$)	0% ($\pm 0.23\%$)	0% ($\pm 0.25\%$)	0% ($\pm 0.00\%$)	0% ($\pm 0.24\%$)
$\overline{E}_{\mathcal{D},m}$	32% ($\pm 0.33\%$)	44% ($\pm 0.10\%$)	22% ($\pm 1.01\%$)	22% ($\pm 0.98\%$)	20% ($\pm 1.03\%$)	32% ($\pm 0.69\%$)	25% ($\pm 1.15\%$)
Parameters	k=3	B=0.05	k=24 (cosine)	k=25 (l_2)	k=1 (cosine)	k=2	-
BER	42%	76%	48%	44%	41%	40%	50%
$\bar{E}_{\mathcal{D},m}$	14% ($\pm 0.16\%$)	35% ($\pm 0.12\%$)	20% ($\pm 0.70\%$)	17% ($\pm 0.56\%$)	20% ($\pm 0.78\%$)	13% ($\pm 1.71\%$)	25% ($\pm 0.91\%$)
$\underline{E}_{\mathcal{D},m}$	7% ($\pm 0.08\%$)	2% ($\pm 0.03\%$)	0% ($\pm 0.24\%$)	0% ($\pm 0.24\%$)	0% ($\pm 0.25\%$)	7% ($\pm 0.76\%$)	0% ($\pm 0.24\%$)
min $\overline{E}_{\mathcal{D},m}$	21% ($\pm 0.23\%$)	37% ($\pm 0.15\%$)	20% ($\pm 0.91\%$)	17% ($\pm 0.77\%$)	20% ($\pm 1.03\%$)	20% ($\pm 2.39\%$)	25% ($\pm 1.15\%$)

Table 4: Full results on *raw* input features of CIFAR100.

	DE-kNN	Gaussian KDE	kNN-LOO	kNN	1NN	1NN-kNN	GHP
Parameters	k=2	B=0.001	k=1 (cosine)	k=1 (cosine)	k=1 (cosine)	k=2	-
min BER	44%	1%	66%	57%	57%	71%	69%
$\bar{E}_{\mathcal{D},m}$	10% ($\pm 0.04\%$)	0% ($\pm 0.00\%$)	30% ($\pm 0.61\%$)	26% ($\pm 0.45\%$)	26% ($\pm 0.45\%$)	30% ($\pm 1.27\%$)	31% ($\pm 0.57\%$)
$\underline{E}_{\mathcal{D},m}$	14% ($\pm 0.04\%$)	48% ($\pm 0.12\%$)	0% ($\pm 0.15\%$)	0% ($\pm 0.13\%$)	0% ($\pm 0.13\%$)	1% ($\pm 0.27\%$)	0% ($\pm 0.15\%$)
$E_{\mathcal{D},m}$	23% ($\pm 0.08\%$)	48% ($\pm 0.12\%$)	30% ($\pm 0.77\%$)	26% ($\pm 0.58\%$)	26% ($\pm 0.58\%$)	31% ($\pm 1.48\%$)	31% ($\pm 0.71\%$)
Parameters	k=2	B=0.001	k=18 (L_2)	k=16 (cosine)	k=1 (cosine)	k=2	-
BER	44%	1%	67%	61%	57%	71%	69%
min $\bar{E}_{\mathcal{D},m}$	10% ($\pm 0.04\%$)	0% ($\pm 0.00\%$)	29% ($\pm 0.54\%$)	24% ($\pm 0.43\%$)	26% ($\pm 0.45\%$)	30% ($\pm 1.27\%$)	31% ($\pm 0.57\%$)
$\underline{E}_{\mathcal{D},m}$	14% ($\pm 0.04\%$)	48% ($\pm 0.12\%$)	0% ($\pm 0.15\%$)	0% ($\pm 0.13\%$)	0% ($\pm 0.13\%$)	1% ($\pm 0.27\%$)	0% ($\pm 0.15\%$)
$E_{\mathcal{D},m}$	23% ($\pm 0.08\%$)	48% ($\pm 0.12\%$)	29% ($\pm 0.69\%$)	24% ($\pm 0.57\%$)	26% ($\pm 0.58\%$)	31% ($\pm 1.48\%$)	31% ($\pm 0.71\%$)
Parameters	k=100	B=0.05	k=22 (cosine)	k=3 (cosine)	k=1 (cosine)	k=10	-
BER	90%	76%	68%	60%	57%	79%	69%
$\bar{E}_{\mathcal{D},m}$	41% ($\pm 0.10\%$)	33% ($\pm 0.53\%$)	29% ($\pm 0.52\%$)	27% ($\pm 0.52\%$)	26% ($\pm 0.45\%$)	39% ($\pm 0.50\%$)	31% ($\pm 0.57\%$)
min $\underline{E}_{\mathcal{D},m}$	0% ($\pm 0.01\%$)	2% ($\pm 0.10\%$)	0% ($\pm 0.15\%$)	0% ($\pm 0.12\%$)	0% ($\pm 0.13\%$)	0% ($\pm 0.00\%$)	0% ($\pm 0.15\%$)
$E_{\mathcal{D},m}$	41% ($\pm 0.10\%$)	35% ($\pm 0.63\%$)	29% ($\pm 0.67\%$)	27% ($\pm 0.64\%$)	26% ($\pm 0.58\%$)	39% ($\pm 0.50\%$)	31% ($\pm 0.71\%$)
Parameters	k=2	B=0.01	k=18 (L_2)	k=16 (cosine)	k=1 (cosine)	k=2	-
BER	44%	27%	67%	61%	57%	71%	69%
$\bar{E}_{\mathcal{D},m}$	10% ($\pm 0.04\%$)	5% ($\pm 0.14\%$)	29% ($\pm 0.54\%$)	24% ($\pm 0.43\%$)	26% ($\pm 0.45\%$)	30% ($\pm 1.27\%$)	31% ($\pm 0.57\%$)
$\underline{E}_{\mathcal{D},m}$	14% ($\pm 0.04\%$)	17% ($\pm 0.37\%$)	0% ($\pm 0.15\%$)	0% ($\pm 0.13\%$)	0% ($\pm 0.13\%$)	1% ($\pm 0.27\%$)	0% ($\pm 0.15\%$)
min $E_{\mathcal{D},m}$	23% ($\pm 0.08\%$)	22% ($\pm 0.51\%$)	29% ($\pm 0.69\%$)	24% ($\pm 0.57\%$)	26% ($\pm 0.58\%$)	31% ($\pm 1.48\%$)	31% ($\pm 0.71\%$)

E EXTENDED EXPERIMENTAL EVALUATION

In this section, we provide additional details about the experimental section and present further in-depth results that are omitted in the main body due to space constraints. Due to runtime complexities of the 1NN-LOO and GHP estimators on large datasets, we execute these only on test sets, whereas 1NN makes use of the entire training and test sets. When setting the distance function for 1NN, we report only the results using cosine dissimilarity, since we observed that it is on par and often better than the Euclidean, L_2 , distance.

E.1 Datasets

Table 5 presents the details of the involved datasets. In order to reproduce the setting in which no training was performed on the (new) downstream task, we need to ensure that transformations are trained on different datasets. Therefore, we exclude ImageNet from the list of evaluated datasets. Nonetheless, `ease.ml/snoopy` is executable on ImageNet in a reasonable runtime, enabled by the provided efficient stream version of our algorithm. We note that for the visual classification tasks, the raw features are the pixel intensities, whereas for the text classification there are no trivial raw representations. One might be tempted to apply a bag-of-words preprocessing, but this usually results in high-dimensional representations (i.e., $> 175K$ for YELP) that are not practical for a real-world system. Moreover, bag-of-words preprocessing transforms the input and might increase the Bayes error.

Table 5: Datasets and state-of-the-art performance on classification tasks. Raw features for NLP tasks do not exist.

Name	Dimension	Classes C	Train / Test Samples	SOTA %
MNIST	784	10	60K / 10K	0.16 ⁶
CIFAR10	3072	10	50K / 10K	0.63 ⁶
CIFAR100	3072	100	50K / 10K	6.49 ⁶
IMDB	N/A	2	25K / 25K	3.79 ⁷
SST2	N/A	2	67K / 872	3.2 ⁷
YELP	N/A	5	500K / 50K	27.80 ⁷

E.2 Feature Transformations

We report all the tested feature transformations for `ease.ml/snoopy`-enabled estimators in Table 6 for computer vision tasks, and in Table 7 for NLP tasks. All pre-trained embeddings can be found using the transformation name and the corresponding source⁸. In case of the HuggingFace Transformers embeddings in Table 7, the *Pooled* version denotes the representation that the embedding outputs for the entire text. For other embeddings from that library, the representation of the text is computed by taking the mean over the representations of individual input tokens. PCA transformations are trained on the training set and applied to both the training and the test set. The inference on the training and the test set is run by batching multiple data points as shown in the last column of the tables. The inference sizes are chosen such that the hardware accelerator is capable of running the inference without running out of memory for each transformation when executed in parallel with the full system. There is no limitation when using the identity transformation (raw), or running PCA, which is executed without any accelerator. In the image domain, pre-trained embeddings assume a fixed-size resolution that might differ from the target image size. We adjust those cases using default resizing methods of either TensorFlow or PyTorch. The *identity* transformation allows us to quantify the difference between the raw data representation and transformed features, albeit only for the vision tasks.

⁶Given by Byerly et al. [5] for MNIST and Kolesnikov et al. [17] for CIFAR10 and CIFAR100.

⁷Given by Yang et al. [40]. The SOTA values for SST2 and YELP are provided on slightly different sizes of training sets.

⁸TensorFlow Hub: <https://tfhub.dev>, PyTorch Hub: <https://pytorch.org/hub>, HuggingFace Transformers: <https://huggingface.co/transformers/> and scikit-learn: <https://scikit-learn.org/>

Table 6: Feature transformations for vision tasks.

Transformation	DIM	Source	Infer. Size
<i>Identity (Raw)</i>	-	-	N/A
PCA ₃₂	32	scikit-learn	N/A
PCA ₆₄	64	scikit-learn	N/A
PCA ₁₂₈	128	scikit-learn	N/A
AlexNet	4096	PyTorch Hub	500
GoogLeNet	1024	PyTorch Hub	500
VGG16	4096	PyTorch Hub	125
VGG19	4096	PyTorch Hub	125
InceptionV3	2048	TensorFlow Hub	250
ResNet50-V2	2048	TensorFlow Hub	250
ResNet101-V2	2048	TensorFlow Hub	250
ResNet152-V2	2048	TensorFlow Hub	250
EfficientNet-B0	1280	TensorFlow Hub	125
EfficientNet-B1	1280	TensorFlow Hub	125
EfficientNet-B2	1408	TensorFlow Hub	125
EfficientNet-B3	1536	TensorFlow Hub	125
EfficientNet-B4	1792	TensorFlow Hub	50
EfficientNet-B5	2048	TensorFlow Hub	25
EfficientNet-B6	2304	TensorFlow Hub	20
EfficientNet-B7	2560	TensorFlow Hub	10

Table 7: Feature transformations for NLP tasks.

Transformation	DIM	Source	Infer. Size
NNLM-en	50	TensorFlow Hub	5000
NNLM-en (With Normalization)	50	TensorFlow Hub	5000
NNLM-en	128	TensorFlow Hub	5000
NNLM-en (With Normalization)	128	TensorFlow Hub	5000
ELMo	1024	TensorFlow Hub	4
Universal Sentence Encoder (USE)	512	TensorFlow Hub	2500
Universal Sentence Encoder (USE) Large	512	TensorFlow Hub	50
BERT Base Cased Pooled (BCP)	768	HuggingFace Transformers	100
BERT Base Uncased Pooled (BUP)	768	HuggingFace Transformers	100
BERT Base Cased (BC)	768	HuggingFace Transformers	100
BERT Base Uncased (BU)	768	HuggingFace Transformers	100
BERT Large Cased Pooled (LCP)	1024	HuggingFace Transformers	50
BERT Large Uncased Pooled (LUP)	1024	HuggingFace Transformers	50
BERT Large Cased (LC)	1024	HuggingFace Transformers	50
BERT Large Uncased (LU)	1024	HuggingFace Transformers	50
XLNet	768	HuggingFace Transformers	25
XLNet Large	1024	HuggingFace Transformers	25

E.3 Extended End-To-End Use Case

In this section we outline the experimental details for the end-to-end use case and provide additional figures supporting the results described in the main body of this work. Due to the requirement of running the lightweight AutoML system and tuning the best LR model for different amount of label noise, we only ran the costly experiments for CIFAR100 and IMDB. All reported values represent the mean (accuracy and run-time) over at least 5 independent runs. The costs represent a hypothetical “dollar price” consisting of two components: (1) the labelling effort performed by human annotators, a hyper-parameter, and (2) the costs of running computation on a single GPU Amazon EC2 instance (at 0.9\$ per hour).

Labeling costs. We consider two different scenarios. On the one hand we assume acquiring labels can be done relatively fast, requiring 5 seconds per label. At an hourly pay-rate of 15 dollars, this results in roughly 0.02 dollars per label. On the other hand, we define a more costly scenario in which labels are acquired with frequency of 1 minute per label. With the same pay-rate, this yields roughly 0.25 dollars per label.

ease.ml/snoopy. When running `ease.ml/snoopy` we define the time needed to reach the lowest 1NN error across all embeddings based on multiple independent runs as described in Section 5.3. This results in a runtime of 0.27 hours for CIFAR100 and 0.69 hours for IMDB on a single GPU. These runtimes include the 1NN computation and running inference, with the latter being the most costly part, particularly for large NLP models. When re-running `ease.ml/snoopy` after having cleaned a fixed portion of the labels (set to 1% of the dataset size) we assume the “best” embedding did not change and, therefore, no additional inference needs to be executed. This assumption holds for both evaluated datasets and would remain comparable to training LR models otherwise as well, as running inference on the datasets using all models (required exactly once) was not considered for the runtime definition of the latter.

1NN Accuracies. Calculating the minimal nearest neighbor accuracy is a direct byproduct of running `ease.ml/snoopy` and therefore has the same computational requirement.

LR Models. As mentioned before, when training the logistic regression models we assume that the representations for all the training and test samples are calculated in advance exactly once. This, sometimes very costly step, is omitted in our analysis. After having cleaned the same fixed portion of labels (1% of test and train samples), re-training the LR models does not require any inference. We train all LR models using SGD with a momentum of 0.9, a mini-batch size of 64 and 200 epochs. We select the minimal test accuracy achieved over all combinations of learning rate in $\{0.0001, 0.001, 0.01, 0.1\}$ and L_2 regularization values in $\{0.0, 0.0001, 0.001, 0.01, 0.1\}$. We calculate the average time needed to train a LR based on the best transformation, without label noise, on all possible hyper-parameters. This amounts to 2.5 hours for CIFAR100 on EfficientNet-B4 features, and 1.3 hours for IMDB on XLNet features. The hyper-parameter search was conducted 5 independent times for 11 linearly sampled values for injected label noise between 0.0 and 1.0.

The LR proxy model accuracies are often comparable to our BER estimations (in fact the largest gap was visible for IMDB among all datasets). The computational difference between both approaches can nevertheless be significant. By overlapping the nearest neighbor computation with running the more costly inference steps, getting \hat{S}_X amounts in the worst case to the sum of the time needed to perform inference on all models of the entire dataset. This can be further optimized as described in the paper. On the other hand, calculating the best LR model requires at least `ease.ml/snoopy`’s worst case run time in order to first get all feature representations. Training and tuning the hyper-parameters then typically requires a multiple of this runtime on top of it, rendering it orders of magnitude more expensive than `ease.ml/snoopy`.

Lightweight AutoML. The goal of the lightweight AutoML system is to replicate the SOTA values achieved for both datasets. Unluckily, this was not possible for either of the datasets mainly due to computational constraints and lack of publicly available reproducible code. We therefore perform our best, mostly manual, efforts to train a model on the original non-corrupted data. For CIFAR100, we fine-tuned the EfficientNet-B4 model based on the setting defined by Tan and Le [37] resulting in a set of 56 different hyper-parameters. The run-time to train those 56 different model on a single GPU is roughly 550 hours. For IMDB, the authors spent multiple days on up to 8 GPUs in order to find which pre-trained model to fine-tune and which settings should be employed in order to achieve a higher accuracy than the best LR model accuracy on *frozen* features. The lack of reproducibility, and mostly the impact of all the hyper-parameters, such as maximal sequence length, the batch size, learning rate strategy, optimizer, number of epochs and other settings, e.g., regularization technique when fine-tuning large language models such as BERT, render the task of defining a lightweight AutoML system very challenging. The best accuracy of nearly 94% was achieved using the BERT Base Uncased model, with maximal sequence length of 512, batch size of 6, one epoch on an initial learning rate of $2e-5$ and the Adam optimizer. Fine-tuning IMDB on a single GPU with exactly those hyper-parameters takes roughly 25 minutes. Clearly, this runtime is not representative for the required runtime of a lightweight AutoML system. We therefore opted to select the same runtime of 550 hours on a single GPU for both datasets.

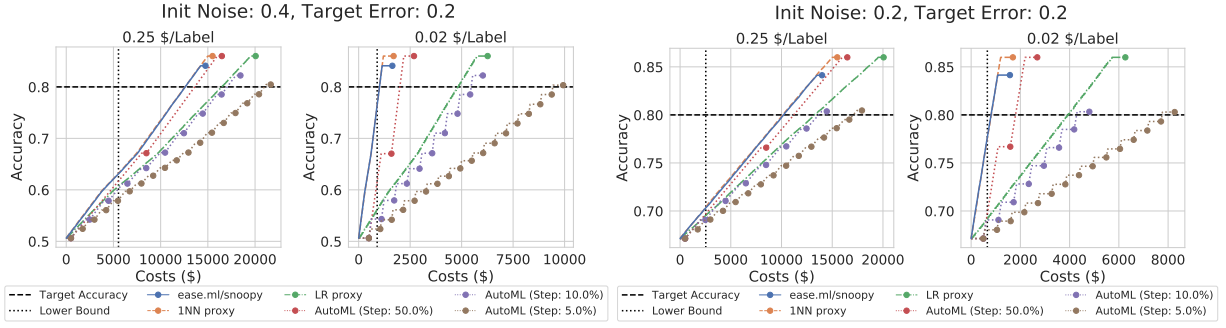


Figure 8: End-to-end label cleaning on CIFAR100. The dots represent trained models accuracies after running AutoML.

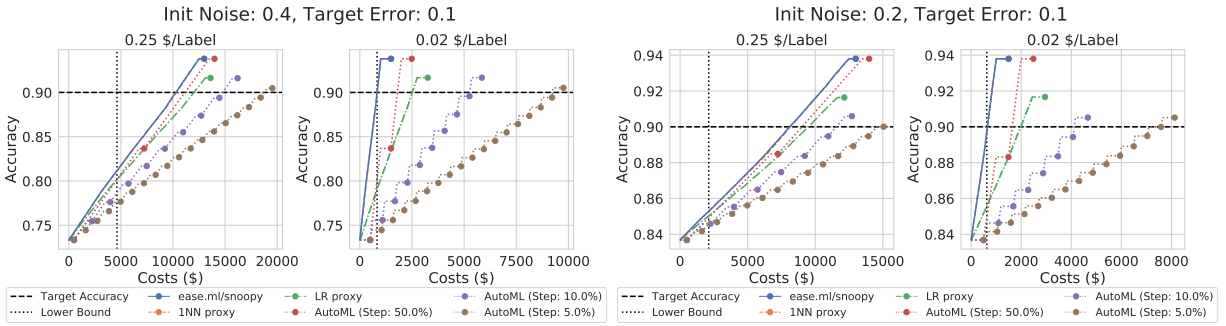


Figure 9: End-to-end label cleaning on IMDB. The dots represent trained models accuracies after running AutoML.

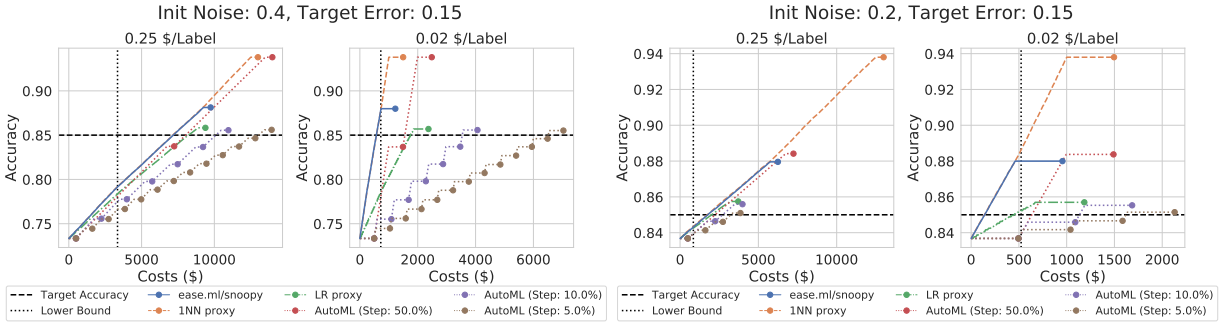


Figure 10: End-to-end label cleaning on IMDB. The dots represent trained models accuracies after running AutoML.

E.4 Estimation Accuracy of ease.ml/snoopy

In this section we provide the evaluation of the 1NN estimator on top of different feature transformations over all datasets. We summarize the results of ease.ml/snoopy on all datasets without label noise in Table 8. We compare the results to the choice of using 1NN-LOO and GHP. We see that both algorithms do not yield any significant improvements over choosing 1NN for all datasets despite being more computationally demanding.

When evaluating the 1NN estimator accuracy for varying label noise, and its convergence under different feature transformations (Figures 11, 12 and 13), we see that even the best transformations are constantly over-estimating the lower bound when increasing label noise, validating the key arguments for taking the minimum over all estimators. Nevertheless, the BER estimator score $E_{\mathcal{D},m}$, mentioned in Section 4 and formally defined in Section D.1, significantly decreases, e.g., from 25.6% ($\sigma = 0.6\%$) using the raw features to 6% ($\sigma = 0.5\%$) using the best embedding for CIFAR100. The convergence plots further validate the convexity assumption of the 1NN estimation with increasing number of samples, used in the improved version of successive-halving in Section 3.3.

All the results indicate the median, 95% and 5% quantiles over multiple independent runs (i.e. 10 for YELP and 30 otherwise). We observe the presence of much more noise in SST2 when compared to other datasets, as seen in Figure 12. This is not at all surprising since SST2 has a very small test set consisting of less than one thousand samples, as seen in Table 5. This naturally results in higher variance and less confidence when estimating the 1NN classifier accuracy compared to the larger number of test samples for the other datasets.

Table 8: BER estimation values, evaluation framework score and minimal transformation for all algorithms suitable for ease.ml/snoopy.

Dataset	SOTA	1NN			1NN-LOO			GHP		
		\widehat{S}_X	$E_{\mathcal{D},m}$	Min. Transformation	\widehat{S}_X	$E_{\mathcal{D},m}$	Min. Transformation	\widehat{S}_X	$E_{\mathcal{D},m}$	Min. Transformation
MNIST	0.16%	1.4%	0.9% ($\pm 0.6\%$)	Raw	1.9%	1.3% ($\pm 0.7\%$)	PCA ₃₂	2.0%	1.3% ($\pm 0.7\%$)	PCA ₃₂
CIFAR10	0.63%	5.2%	2.5% ($\pm 0.6\%$)	EfficientNet-B4	6.7%	3.4% ($\pm 0.9\%$)	EfficientNet-B4	6.8%	3.5% ($\pm 0.8\%$)	EfficientNet-B4
CIFAR100	6.49%	18.2%	6.0% ($\pm 0.5\%$)	EfficientNet-B5	22.9%	8.3% ($\pm 0.6\%$)	EfficientNet-B4	24.2%	8.9% ($\pm 0.6\%$)	EfficientNet-B4
IMDB	3.79%	10.8%	3.9% ($\pm 0.7\%$)	XLNet	9.1%	2.9% ($\pm 0.7\%$)	XLNet	10.5%	3.6% ($\pm 0.7\%$)	BERT Large Uncased
SST2	3.2%	13.4%	6.3% ($\pm 2.1\%$)	BERT Large Uncased	17.3%	8.2% ($\pm 2.7\%$)	BERT Large Cased	17.8%	8.5% ($\pm 2.7\%$)	USE Large
YELP	27.80%	27.2%	0.4% ($\pm 0.4\%$)	XLNet	28.4%	0.5% ($\pm 0.4\%$)	BERT Large Uncased	28.8%	0.7% ($\pm 0.4\%$)	BERT Large Uncased

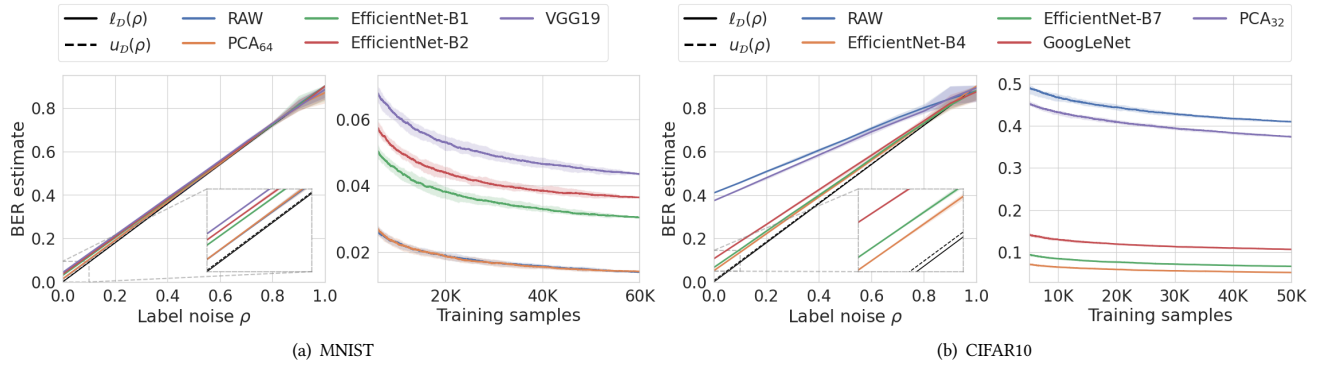


Figure 11: Evaluation and convergence of 1NN estimator for different feature transformations. (Left each) All the training points for different amount of label noise. (Right each) Zero label noise and increasing number of training samples.

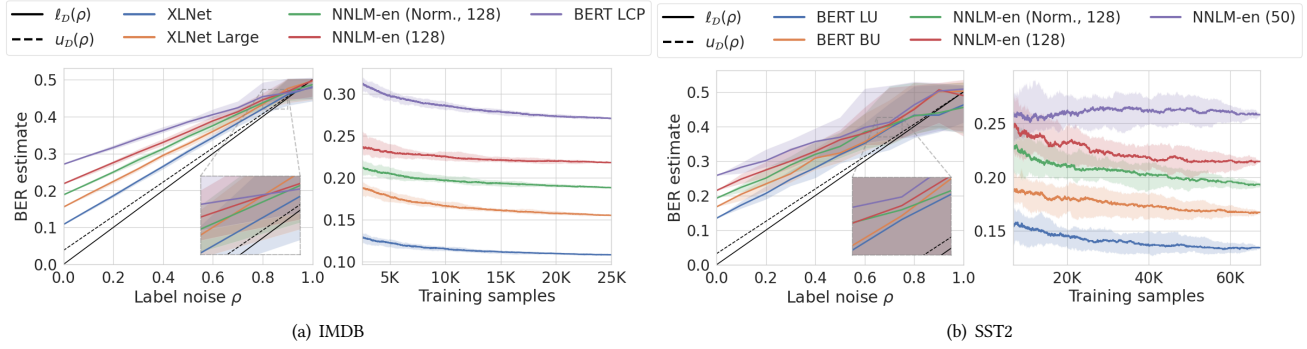


Figure 12: Evaluation and convergence of 1NN estimator for different feature transformations. (Left each) All the training points for different amount of label noise. (Right each) Zero label noise and increasing number of training samples.

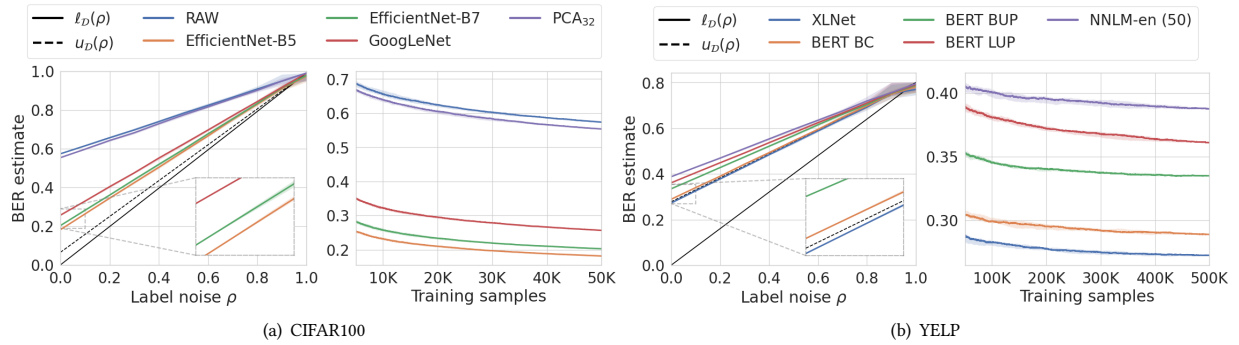


Figure 13: Evaluation and convergence of 1NN estimator for different feature transformations. (Left each) All the training points for different amount of label noise. (Right each) Zero label noise and increasing number of training samples.